CHAPTER 5

RESULTS AND CALCULATIONS

5.1 Thermal Characterisation before Melt Spinning

5.1.1 Polypropylene

Thermal characterisation of a polymer prior to processing provides essential information upon which to base a decision about what the appropriate processing temperature should be. In this work, the melting and thermal degradation ranges of the polypropylene beads were determined by differential scanning calorimetry (DSC) and thermogravimetry (TG) respectively. The DSC and TG thermograms are shown in Figs. 5.1 and 5.2.

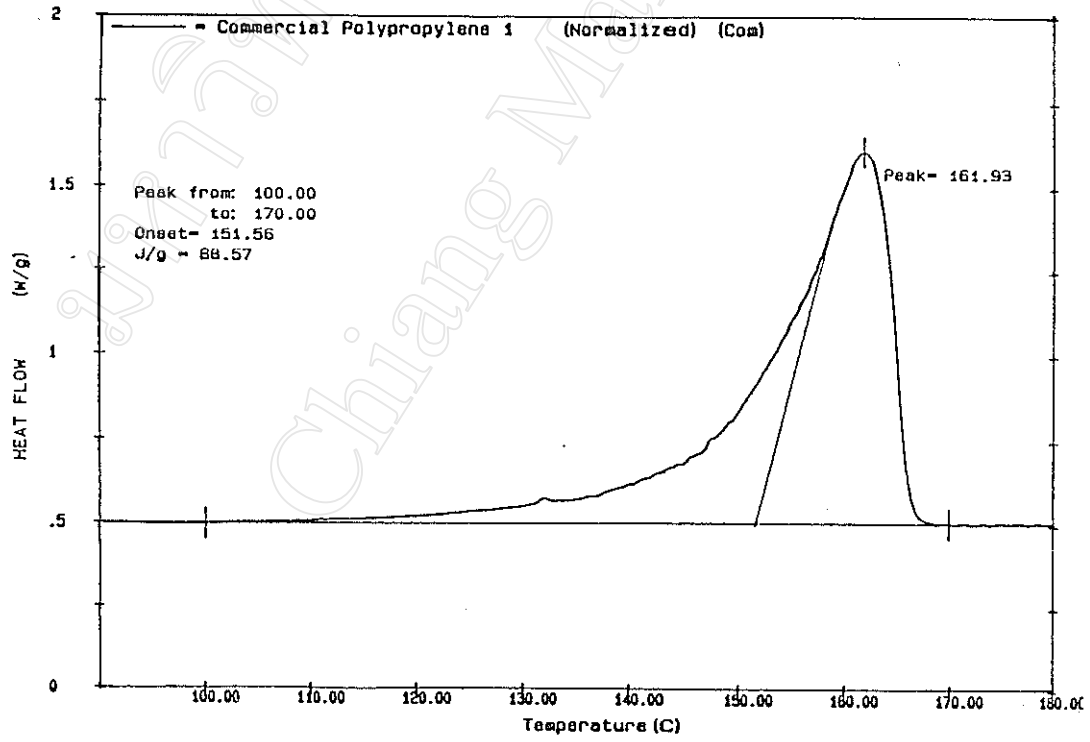

Fig. 5.1 DSC thermogram of the polypropylene beads.

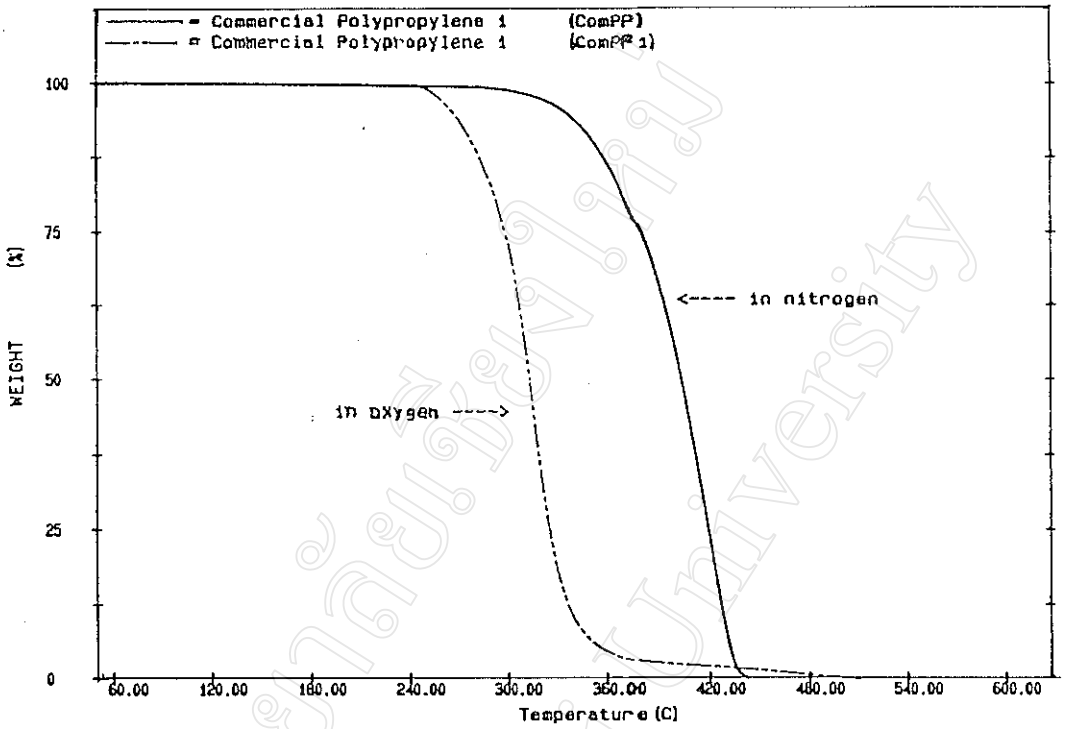

Fig. 5.2 TG thermograms of the polypropylene beads showing the polymer's relative thermal stabilities in nitrogen and oxygen atmospheres.

From the DSC thermogram, it was found that the main melting range was approximately 150-167°C with the peak maximum at 162°C. In addition, the TG thermograms show that the polypropylene starts to degrade at about 290°C under a nitrogen atmosphere but at about 250°C under an oxygen atmosphere. The reason for this difference in thermal stabilities is that, in polypropylene, each alternate carbon atom in the polymer chain bears a tertiary hydrogen atom which is relatively labile. This makes polypropylene prone to attack by oxidizing agents, of particular significance in the processing context being oxidation by air at elevated temperature [46]. In this work, in the melt spinning process, the polypropylene was exposed to the air which contains about 20% oxygen. However, since the polypropylene used was a commercial grade, it can be expected to contain a small amount of antioxidant to act as a thermal stabiliser during processing.

From this combined DSC/TG data, the polymer's "processing window" for melt spinning would, as an approximate guide, normally be considered to be:

processing window = $(T_{m\ max} + 10°C)$ - $(T_{d\ min} - 50°C)$

thus, in a N_2 atmosphere : processing window ≈ 180 - 240°C
while in a O_2 atmosphere : processing window ≈ 180 - 200°C

The recommended melt spinning temperature for polypropylene, as used in this work, was 205°C [34]. At this temperature setting, the molten polymer would normally start to emerge from the spinnerette within the range 200-210°C. Although this would seem to be slightly outside the "processing window" of 180 - 200°C in a (pure) O_2 atmosphere, it should also be taken into account that (a) air contains only 20% O_2 and (b) the polymer contains an antioxidant. Hence, it is unlikely that significant thermal degradation of the polymer would occur between 200 - 210°C, provided that the polymer's "residence time" inside the heated cylinder is not excessively long.

5.1.2 Poly(L-lactic acid-co-ε-caprolactone)

The DSC and TG thermograms of the two poly(L-lactic acid-co-ε-caprolactone) samples studied are shown in Figs. 5.3 - 5.6. As would be expected, the 8:2 copolymer has a higher and narrower melting range than the 7:3 copolymer because of its lower caprolactone content and, therefore, lower degree of structural randomization.

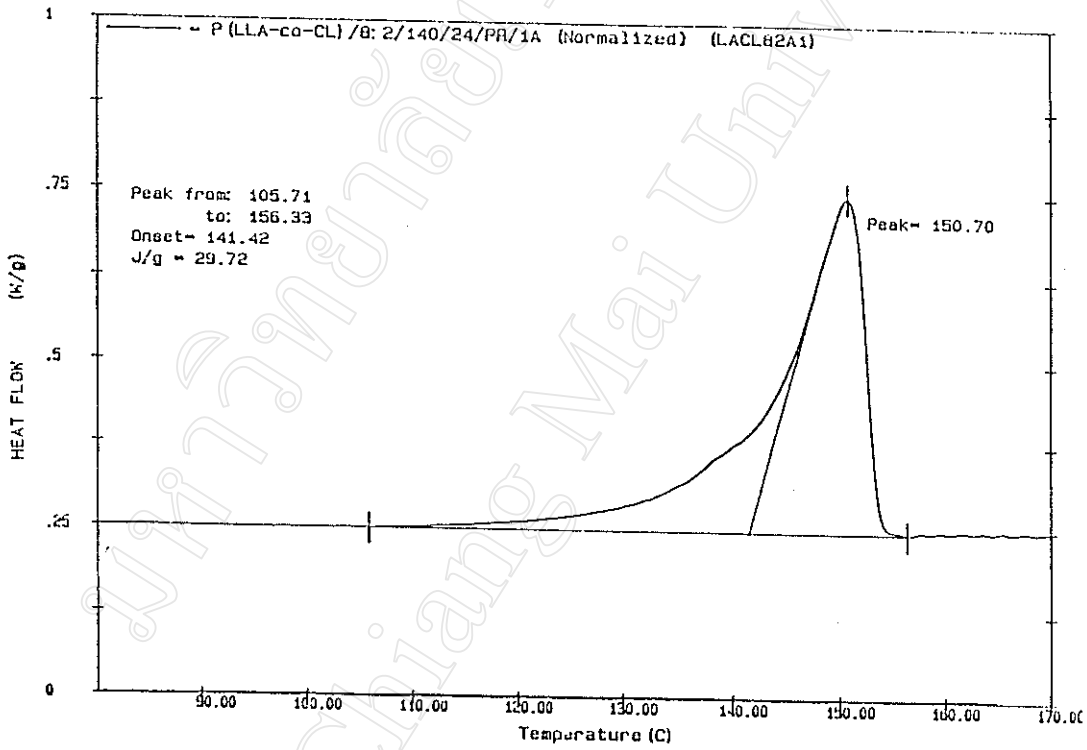

Fig. 5.3 DSC thermogram of poly(L-lactic acid-co-ε-caprolactone) 8:2.

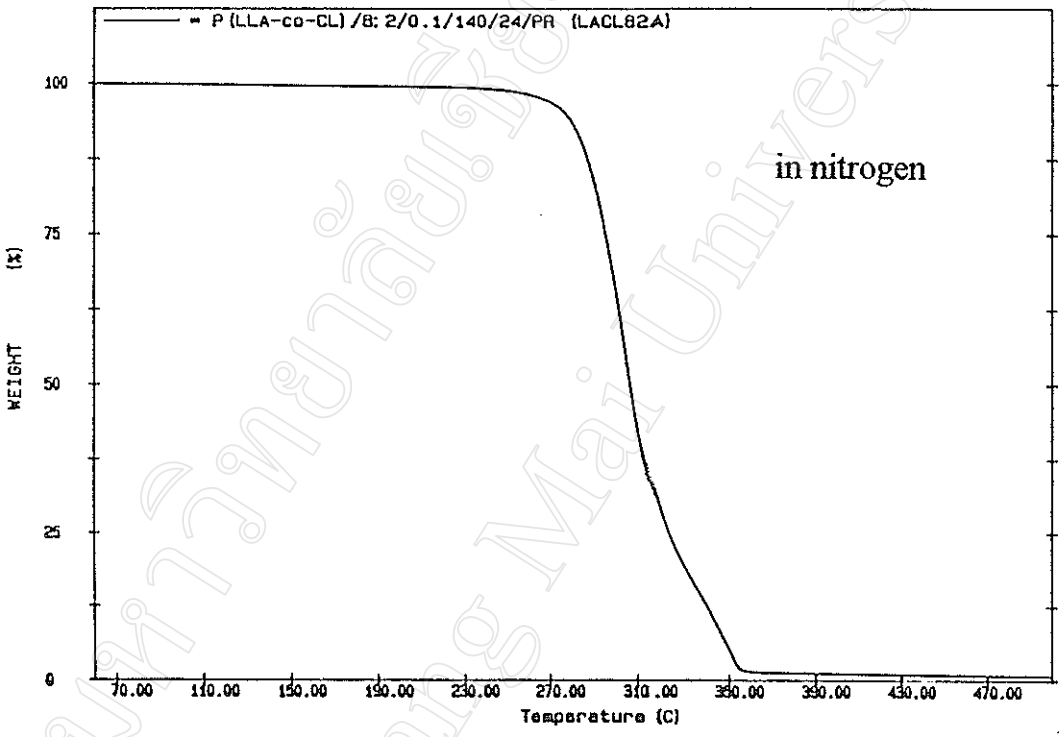

Fig. 5.4 TG thermogram of poly(L-lactic acid-co-ε-caprolactone) 8:2.

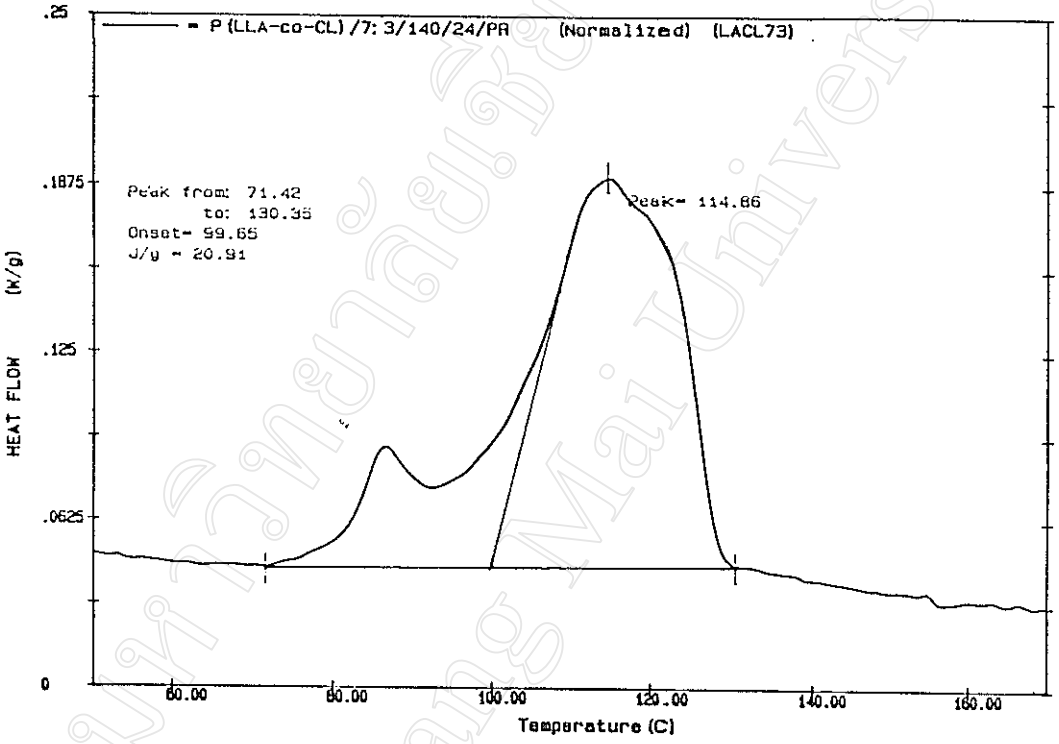

Fig. 5.5 DSC thermogram of poly(L-lactic acid-co-ε-caprolactone) 7:3.

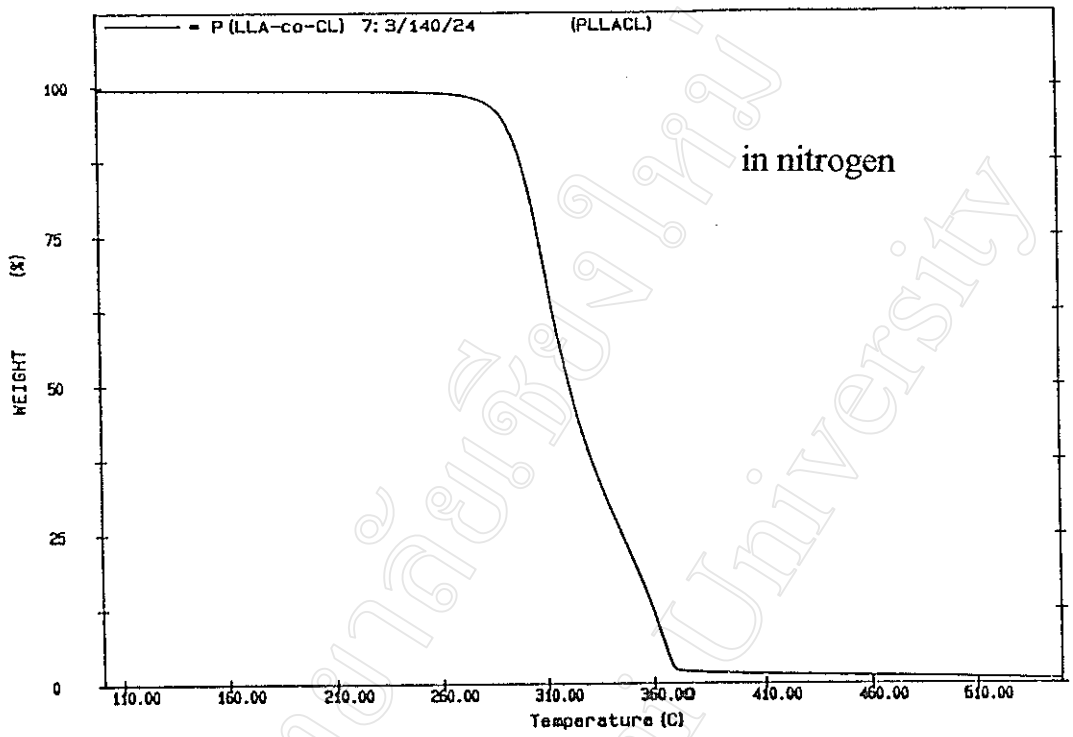

Fig. 5.6 TG thermogram of poly(L-lactic acid-co-ε-caprolactone) 7:3.

Thus, the melt spinning "processing windows" for the two poly(L-lactic acid-co-ε-caprolactone) samples of different compositions are estimated as being:

poly(L-lactic acid-co-ε-caprolactone) 8:2 ≈ 165 - 200°C
poly(L-lactic acid-co-ε-caprolactone) 7:3 ≈ 140 - 190°C

The exact choice of processing temperature within the available range is usually governed by the polymer's rheological properties, especially its melt viscosity. As a general rule, the lowest temperature possible should be used at which the filament thread emerges smoothly and uniformly from the spinnerette without necking or breaking under its own weight before take-up. On this basis, and following a series of trial runs, the actual processing

temperatures used for the two samples were the same (but at different ram speeds - see Table 5.5 in Section 5.3.2):

poly(L-lactic acid-co-ε-caprolactone) 8:2 = 164 - 167°C
poly(L-lactic acid-co-ε-caprolactone) 7:3 = 164 - 167°C

The melt viscosities of the two copolymers were much less than that of polypropylene, resulting in them having quite different rheologies and extrudabilities. This was mainly due to their much lower molecular weights.

5.2 Pre-Formed Polymer Rods

5.2.1 Polypropylene

When the polypropylene rods were being prepared, the heating temperature was set below the lower limit of the polymer's melting range (i.e., <150°C) so that the polymer beads would soften and stick together but not melt. The temperatures used to make the pre-formed rods were 100°C, 120°C, 130°C, 140°C and 145°C. It was found that as the temperature increased the beads could soften, stick together, and compact more easily, thus giving rise to rods with a smoother outer surface. Polypropylene rods pre-formed at each of the above temperatures are shown in Fig. 5.7.

From the results obtained, a temperature of 145°C was chosen as the most suitable temperature for pre-forming polypropylene rods for subsequent use in melt spinning. At this temperature, the rods were smooth and firm, although the outlines of the fused beads were still clearly visible.

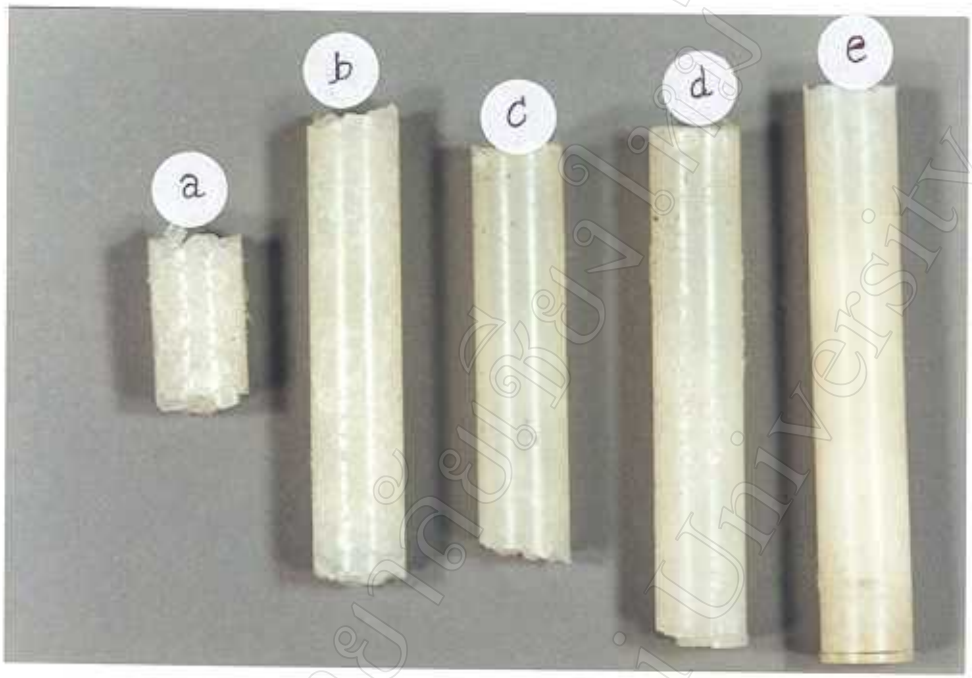

Fig. 5.7 Polypropylene rods pre-formed at various temperatures.

(a) 100°C (b) 120°C (c) 130°C (d) 140°C (e) 145°C

5.2.2 Poly(L-lactic acid-co-ε-caprolactone)

In this research project, the two poly(L-lactic acid-co-ε-caprolactone) copolymers could not be made into pre-formed rods because there was not enough material to do so. Instead, the purified polymer obtained from synthesis was used directly for melt spinning.

5.3 Melt Spinning

5.3.1 Polypropylene

The range of processing conditions used for the melt spinning of polypropylene were as given in Table 5.1.

Table 5.1 Processing conditions used for the melt spinning of polypropylene.

Room temperature = 25.0 ± 1.0°C

Ram Speed (mm/min)	Take-up* Speed (m/min)	Spin-Draw** Ratio (SDR)	Spinning Temperature (°C)	Load Output (kg)
4.00	5.00	5	205	56
3.50	5.00	6	205	52
3.00	5.00	7	205	54
2.50	5.00	8	205	52
2.00	5.00	11	205	54
3.00	10.00	14	205	56
3.00	15.00	21	205	54
3.00	20.00	28	205	52

* also referred to as the "winding speed"

** for method of calculation, see following page

Calculation of the Spin-Draw Ratio (SDR)

The method of calculation of the spin draw-ratio is as follows:

The internal volume (V) of the extrusion cylinder is given by $\pi r^2 h$

$$V = \pi r^2 h$$

Since the volume of the molten polymer inside the cylinder displaced by the piston equals the volume of the polymer exiting from the spinnerette

extrusion volume (inside the cylinder), $\pi r^2_1 h_1$/min = extrudate volume exiting from the spinnerette, $\pi r^2_2 h_2$/min

Example: for melt spinning at a ram speed of 3 $mm.min^{-1}$ and a take-up speed of 5 $m.min^{-1}$ (i.e., condition 3 in Table 5.1)

$$\pi r^2_1 h_1 = \pi r^2_2 h_2$$

where r_1 = internal radius of the cylinder = 7.70 mm
r_2 = radius of the spinnerrette = 0.50 mm
h_1 = the distance that the piston moves per min (ram speed)
= 3.00 $mm.min^{-1}$
h_2 = the length of the extrudate exiting from the spinnerette per min = ?

Then

$$h_2 = \frac{r_1^2 h_1}{r_2^2}$$

$$= \frac{(7.70\ mm)^2 (3.00\ mm.min^{-1})}{(0.5\ mm)^2}$$

$$= 711\ mm.min^{-1}$$

From the definition of the spin-draw ratio (SDR) as the ratio of the take-up speed to the speed of the extrudate exiting from the capillary [10]:

$$\text{spin-draw ratio (SDR)} = \frac{\text{take-up speed}}{\text{extrudate speed, } h_2}$$

$$= \frac{5000 \text{ mm.min}^{-1}}{711 \text{ mm.min}^{-1}}$$

$$\approx 7$$

5.3.1.1 With Thermal Conditioning Zone (TCZ)

In this study, the temperature profile of the filament threadline was modified by passing it through a heating column before take-up. This was aimed at slowing down the rate of cooling, thereby affecting the filaments crystallization kinetics and structure formation. The heating column therefore served as a thermal conditioning zone (TCZ). The effect of temperature profile in the TCZ was also studied; the 3 different profiles employed are given in Tables 5.2 - 5.4. All other processing conditions were kept constant, as detailed below:

Processing Conditions

spin-draw ratio = 7
spinning temperature = 205°C
load output = 101 ± 1 kg
room temperature = 25.0°C ± 1.0°C

Table 5.2 Temperature profile 1 (TCZ1) in the thermal conditioning zone.

Distance from the top of the heating column (± 0.5 cm)	Temperature (°C)
5.0	153.5 ± 0.1
17.0	135.6 ± 0.5
27.0	113.5 ± 0.2
37.0	91.5 ± 0.1
49.0	53.8 ± 1.4

Table 5.3 Temperature profile 2 (TCZ2) in the thermal conditioning zone.

Distance from the top of the heating column (± 0.5 cm)	Temperature (°C)
5.0	130.1 ± 0.2
17.0	111.4 ± 0.1
27.0	93.7 ± 0.2
37.0	75.7 ± 0.2
49.0	46.2 ± 2.2

Table 5.4 Temperature profile 3 (TCZ3) in the thermal conditioning zone.

Distance from the top of the heating column (± 0.5 cm)	Temperature (°C)
5.0	110.6 ± 0.2
17.0	92.7 ± 0.1
27.0	78.4 ± 0.1
37.0	60.2 ± 0.1
49.0	37.7 ± 1.3

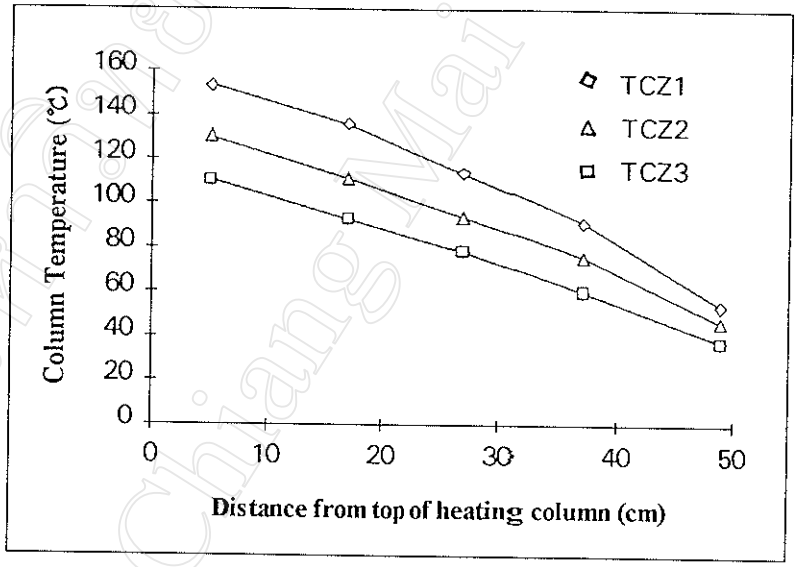

Fig. 5.8 Graphs showing the 3 temperature profiles employed in the temperature conditioning zone (TCZ).

5.3.2 Poly(L-lactic acid-co-ε-caprolactone)

The melt spinning conditions used for poly(L-lactic acid-co-ε-caprolactone) were as listed in Table 5.5.

Table 5.5 Processing conditions used for the melt spinning of the poly(L-lactic acid-co-ε-caprolactone) copolymers.

Copolymer Composition* (LLA : CL mole ratio)	Weight of Copolymer (g)	Spinning Temperature (°C)	Ram Speed ($mm.min^{-1}$)	Load Output (kg)
8:2	2.30	164-167	4.00	16
7:3	5.80	164-167	5.00	30

* approximately equal to the comonomer mole ratios used in synthesis

After melt spinning at different spin-draw ratios, the diameters of the monofilaments were measured by a micrometer. The results for the polypropylene samples are given in Table 5.6. In the case of the poly(L-lactic acid-co-ε-caprolactone) monofilaments, it was found that they were non-uniform in diameter (0.185 ± 0.155 mm) due to their low melt viscosities enabling necking to occur easily (see Fig. 5.9).

Fig. 5.9 Photomicrographs of typical melt spun poly(L-lactic acid-co-ε-caprolactone) monofilaments showing the effects of necking (magnification x 10).

5.4 Off-line Hot Drawing

The polypropylene monofilaments were further drawn off-line at various draw ratios. The off-line draw ratios (OLDR) of each monofilament were calculated using the following definition [9]:

$$\text{Off-line Draw Ratio} = \frac{l_d}{l_u}$$

where l_u is the monofilament length before off-line hot drawing
l_d is the monofilament length after off-line hot drawing

Calculation of the Off-Line Draw Ratio (OLDR)

If the monofilament take-up speeds are:

BEFORE off-line hot drawing = 5 $m.min^{-1}$
AFTER off-line hot drawing = 40 $m.min^{-1}$

Then, the off-line draw ratio $= \frac{40\ m.min^{-1}}{5\ m.min^{-1}}$

OLDR = 8

In this research project, polypropylene monofilaments of all spin-draw ratio (SDR - see Table 5.1) were further drawn off-line at an OLDR of 8 and drawing temperature = 120°C. Also, the effect of varying the OLDR = 2, 4, 6 and 8, at three different temperatures: 100°C, 110°C and 120°C was studied. It was found that when the monofilaments from the melt spinning step were further hot-drawn off-line, their tensile strength increased as their diameter decreased. The average diameters of the monofilaments before off-line hot drawing is show in Table 5.6.

Table 5.6 Average diameters of the polypropylene monofilaments of various spin-draw ratios before off-line hot drawing.

Spin-Draw Ratio (SDR)	Average Monofilament Diameter (mm) ± 0.01
	BEFORE off-line hot drawing
5	0.42
6	0.40
7	0.37
8	0.34
11	0.29
14	0.25
21	0.21
28	0.19
7 (TCZ1)	0.37
7 (TCZ2)	0.37
7 (TCZ3)	0.37

5.5 Thermal Analysis After Melt Spinning

5.5.1 Differential Scanning Calorimetry

5.5.1.1 Polypropylene

The % crystallinities of the polypropylene monofilaments were determined by differential scanning calorimetry (DSC) using the following equation [47].

$$\% \text{ crystallinity, } \chi_c = \frac{\Delta H_s}{\Delta H^*} \times 100\%$$

where ΔH_s = the measured heat of fusion of the sample

ΔH^* = the heat of fusion of a 100% crystalline sample

For polypropylene; $\Delta H^* = 209\ J.g^{-1}$ (from the "Polymer Handbook" [48])

Sample Calculation of the % Crystallinity

Taking the polypropylene monofilament with a spin-draw ratio of 5 (SDR 5) as an example, from its DSC thermogram, as shown in Fig. 5.10, it was found that $\Delta H_s = 83.76\ J.g^{-1}$ (proportional to the area under the crystalline melting endotherm).

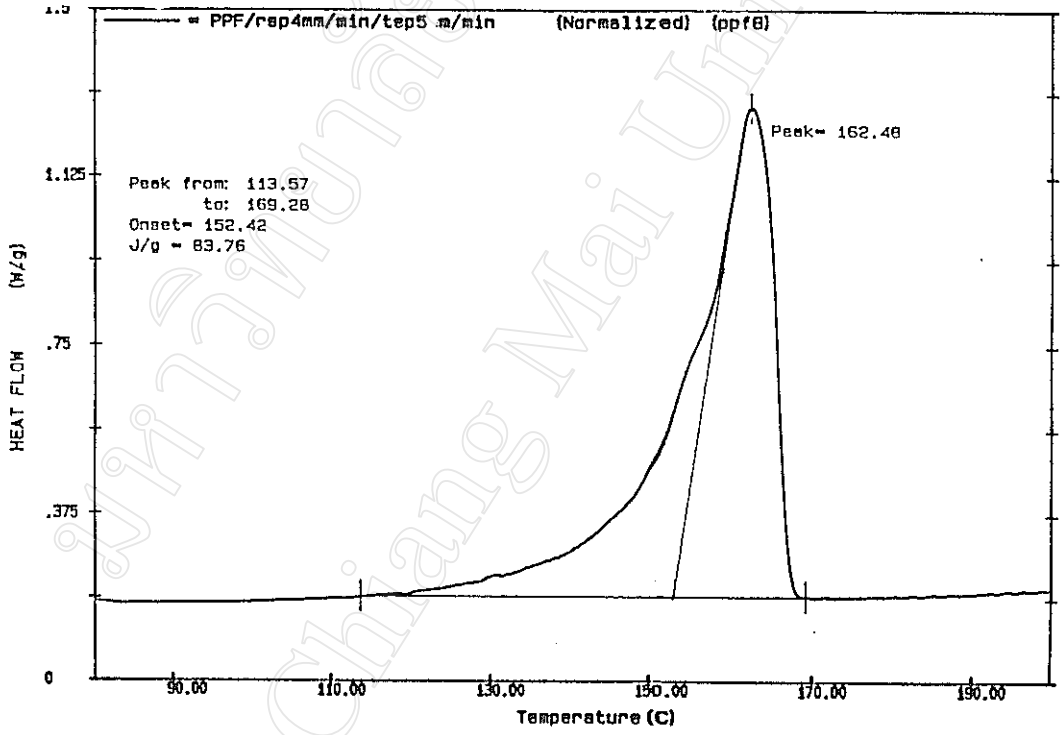

Fig. 5.10 DSC thermogram of polypropylene monofilament SDR 5 showing the melting peak endotherm used in computing the heat of fusion.

Therefore $$\% \text{ crystallinity, } \chi_c = \frac{83.76}{209} \times 100\%$$

$$= 40.1\%$$

The % crystallinities of the polypropylene monofilaments produced at other spin-draw ratios were calculated similarly and their values are compared in Table 5.7.

Table 5.7 Heats of fusion and % crystallinities of the polypropylene monofilaments at various spin-draw ratios (SDR).

SDR	Heat of Fusion ($J.g^{-1}$)	% Crystallinity	T_m* (°C)
5	83.76	40.1	162.48
6	82.57	39.5	162.46
7	83.64	40.0	164.08
8	86.09	41.2	163.75
11	81.47	39.0	163.16
14	83.82	40.1	163.12
21	86.09	41.2	163.75
28	85.07	40.7	162.51
7 (TCZ1)	84.34	40.4	165.46
7 (TCZ2)	83.13	39.8	165.18
7 (TCZ3)	82.54	39.5	165.64

* the melting peak maximum temperature from the DSC curve

cf., for the commercial polypropylene pellets before melt spinning

$$\% \text{ crystallinity} = 42.4\%$$

$$\text{peak } T_m = 161.93°C$$

As the results in Table 5.7 show, neither spin-drawing (SDR) nor thermal conditioning (TCZ) of the monofilaments under the conditions used in this work appear to have had any significant effect on the polymer's % crystallinity. The possible reasons for this will be discussed in the following Chapter 6.

Table 5.8 Heats of fusion and % crystallinities of the polypropylene monofilaments at various spin-draw ratios (SDR) and a subsequent off-line draw ratio (OLDR) of 8; off-line hot drawing (OLHD) temperature = 120°C.

SDR	OLDR	Heat of Fusion ($J.g^{-1}$)	% Crystallinity	T_m* (°C)
5	-	83.76	40.1	162.48
5	8	94.93	45.4	163.04
6	8	97.32	46.6	164.44
7	8	98.26	47.0	161.19
8	8	95.14	45.5	160.19
11	8	97.72	46.8	160.79
14	8	93.96	45.0	160.76
21	8	98.92	47.3	160.67
28	8	97.19	46.5	161.38
7 (TCZ1)	8	99.04	47.4	165.17
7 (TCZ2)	8	90.34	43.2	161.88
7 (TCZ3)	8	95.15	45.5	163.90

* the melting peak maximum temperature from the DSC curve

Table 5.9 Heats of fusion and % crystallinities (χ_c) at various off-line draw ratios (OLDR) and off-line hot drawing temperatures (T_{OLHD}) for the polypropylene monofilament SDR 7.

OLDR	T_{OLHD} = 100°C		T_{OLHD} = 110°C		T_{OLHD} = 120°C	
	ΔH_f (J/g)	χ_c (%)	ΔH_f (J/g)	χ_c (%)	ΔH_f (J/g)	χ_c (%)
2	89.37	42.8	88.67	42.4	86.69	41.5
4	87.69	42.0	86.47	41.4	94.73	45.3
6	94.06	45.0	83.99	40.2	92.39	44.2
8	96.25	46.1	95.53	45.7	98.26	47.0

Typical DSC thermograms of the spin-drawn and spin-drawn/off-line hot drawn polypropylene monofilaments are compared in Fig. 5.11.

Comparison of the DSC thermograms in Fig. 5.11 shows that off-line hot drawing does have an effect on the melting characteristics of the polymer. Two melting peak maxima are observed in the thermogram of the off-line hot drawn sample instead of one. This indicates that off-line hot drawing in the solid state is more effective at inducing further crystallisation than spin-drawing in the melt state.

Finally, the effect of annealing (static heat treatment) on the spin-drawn/off-line hot drawn (SDR 7, OLDR 8) was also studied. Annealing can often improve the mechanical properties of a fibre by increasing the polymer molecular weight and/or crystal perfection. Again, DSC can be conveniently used to estimate quantitatively the change in crystallinity. Fig. 5.12 illustrates the DSC thermogram of one of the annealed polypropylene monofilaments.

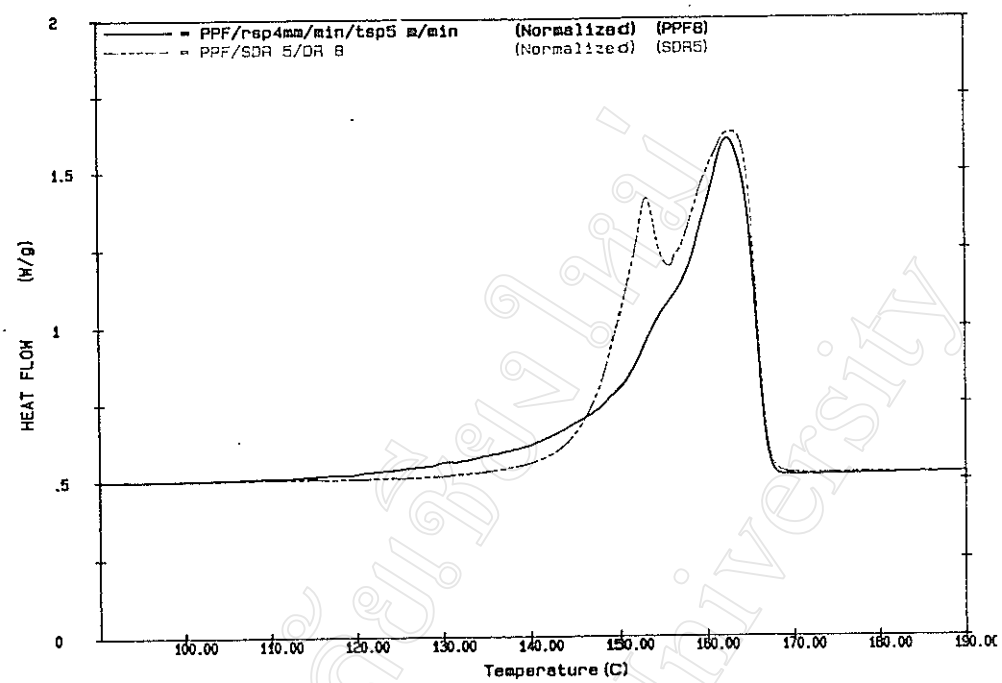

Fig. 5.11 Comparison of the DSC thermograms of spin-drawn (SDR 5) and spin-drawn/off-line hot drawn (SDR 5, OLDR 8) polypropylene monofilaments.

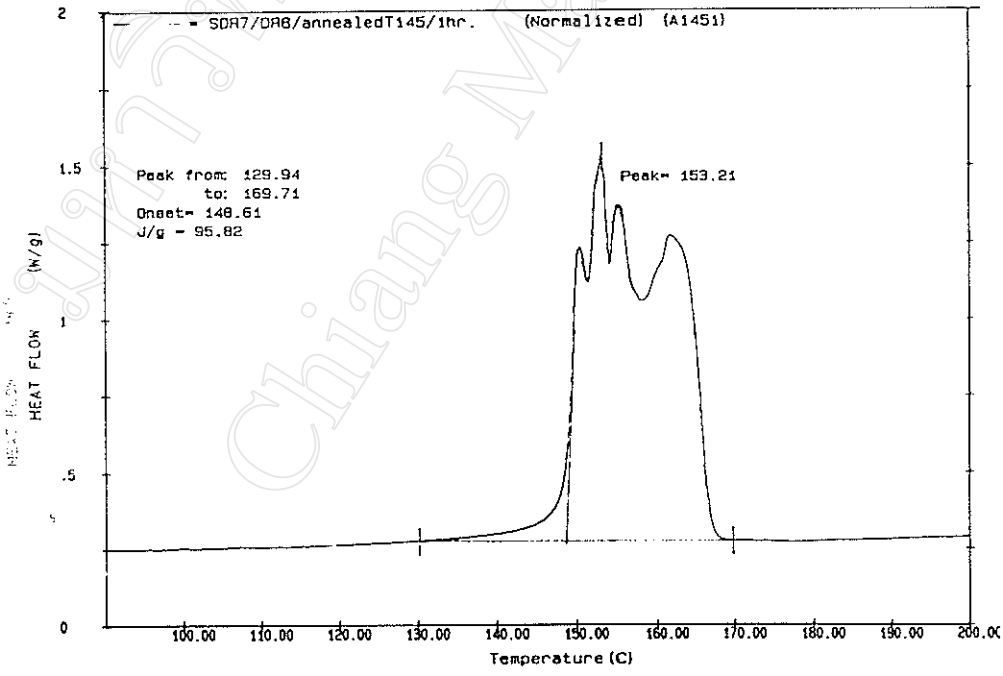

Fig. 5.12 DSC thermogram of the annealed polypropylene (SDR 7, OLDR 8) monofilament; annealing temperature = 145°C and annealing time = 1 hour.

The heat of fusions and % crystallinities of the polypropylene monofilaments (SDR 7 and OLDR 8) annealed at three different temperatures (145°C, 150°C and 155°C) for 1 and 5 hours are compared in Table 5.10.

Table 5.10 Heats of fusion and % crystallinities of polypropylene monofilaments (SDR 7 and OLDR 8) annealed at various temperatures and for different times.

Temp. (°C)	1 hr.		5 hrs.	
	ΔH_f (J/g)	χ_c (%)	ΔH_f (J/g)	χ_c (%)
145	95.82	45.85	93.15	44.74
150	96.18	46.02	91.01	43.54
155	91.88	43.96	104.89	50.17

% crystallinity of the corresponding polypropylene monofilament (SDR 7, OLDR 8) before annealing = 47.0%

The annealing temperatures were chosen from within a range slightly below the onset T_m, as shown in the DSC curve. At these temperatures, the thermal energy and, hence, the molecular motion within the polymer is sufficient to allow solid-state molecular rearrangement to occur leading to further crystallisation. However, this is a time-dependent as well as a temperature-dependent process and it would appear from the results in Table 5.10 that increased crystallisation has only taken place after annealing at the highest temperature (155°C) for the longest time (5 hrs.). It is also possible, of course, that the polypropylene monofilament before annealing was already as crystalline as it could be and so there was little scope left for further crystallisation to take place.

5.5.1.2 Poly(L-lactic acid-co-ε-caprolactone)

The DSC thermograms in Fig. 5.13 compare the melting behaviour of the synthesized poly(L-lactic acid-co-ε-caprolactone) 8:2 copolymer before and after melt spinning.

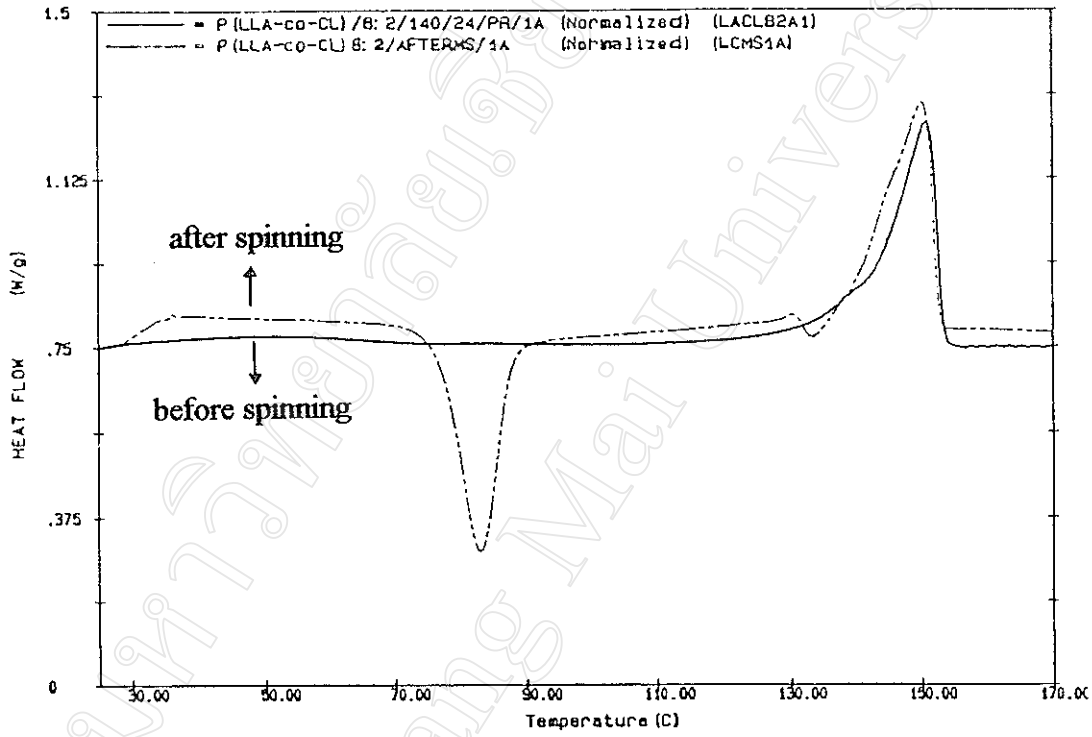

Fig. 5.13 Comparison of the DSC thermograms of the synthesized poly(L-lactic acid-co- ε-caprolactone) 8:2 copolymer sample before and after melt spinning.

As shown in Fig. 5.14, the poly(L-lactic acid-co-ε-caprolactone) 8:2 monofilament exhibited a clear exothermic crystallisation peak after melt spinning. This evidence indicated that when the molten polymer emerged from the spinnerette, it was quenched by the cool air. This resulted in the morphology of the monofilament being in the quenched amorphous state so that, when it was re-heated in the DSC, crystallisation occurred prior to melting. The significance of this will be discussed in more detail in the next chapter.

Fig. 5.14 compares the DSC thermograms of the melt spun poly(L-lactic acid-co-ε-caprolactone) 8:2 monofilament before and after annealing. As expected, annealing at a temperature just below the copolymer's onset T_m also resulted in crystallisation, as shown in Fig. 5.14 by the disappearance of the crystallisation exotherm.

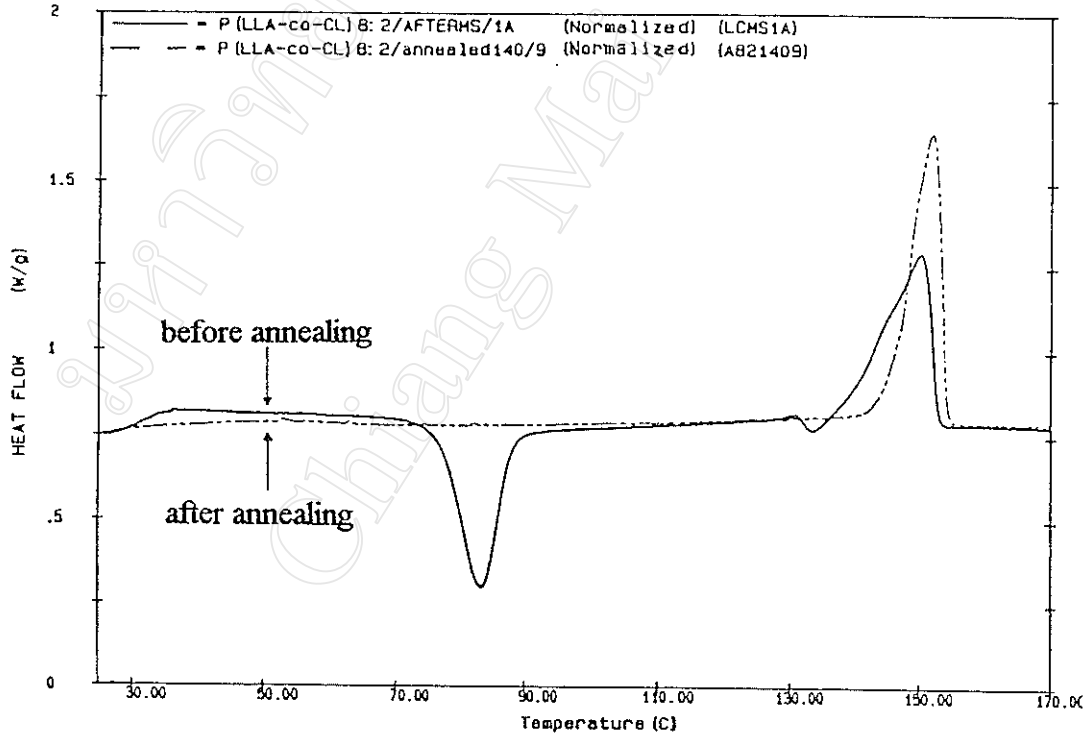

Fig. 5.14 Comparison of the DSC thermograms of the poly(L-lactic acid-co-ε-caprolactone) 8:2 monofilament before and after annealing; annealing temperature = 140°C, annealing time = 9 hours.

The DSC thermograms of the poly(L-lactic acid-co-ε-caprolactone) 7:3 copolymer are shown in Fig. 5.15. The change in monofilament morphology following annealing is not so marked as in the case of the 8:2 copolymer because of the much lower level of crystallinity. The 7:3 copolymer has a more randomised monomer sequence distribution and is therefore less able to crystallise.

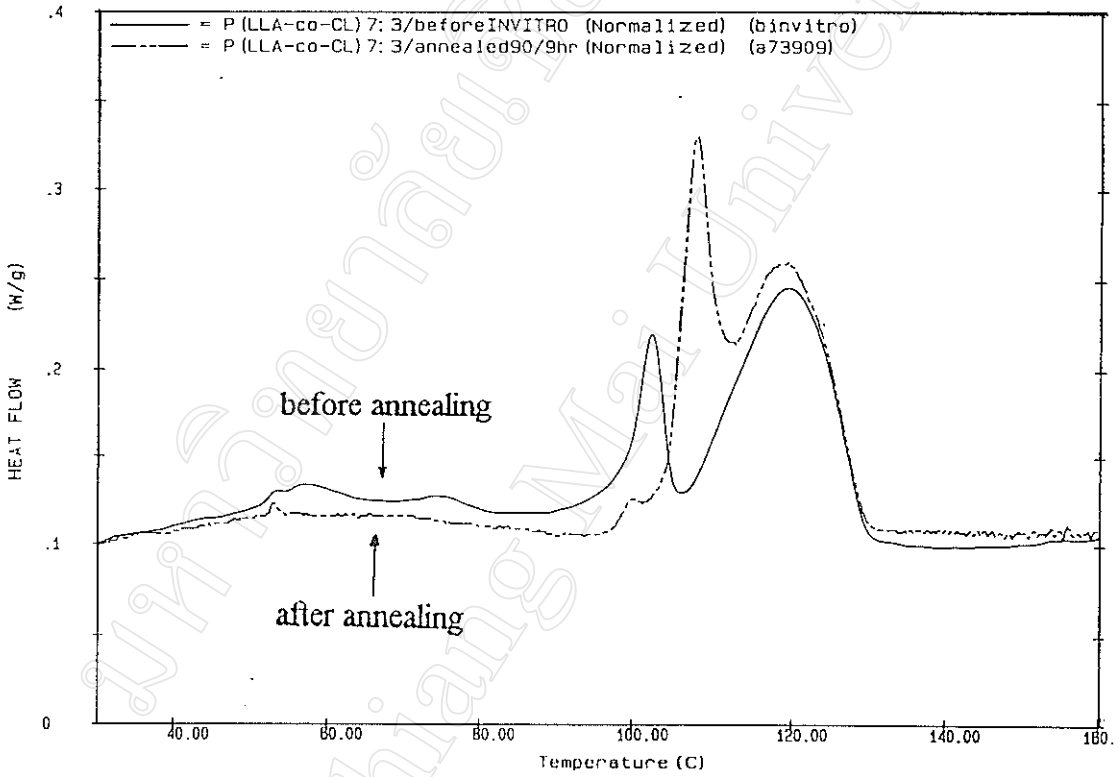

Fig. 5.15 Comparison of the DSC thermograms of the poly(L-lactic acid-co-ε-caprolactone) 7:3 monofilament before and after annealing annealing temperature = 90°C, annealing time = 9 hours.

From the DSC thermograms, the heats of fusion and melting temperatures of the poly(L-lactic acid-co-ε-caprolactone) 8:2 and 7:3 samples are summarized in Table 5.11.

Table 5.11 Data obtained from the DSC thermograms of the poly(L-lactic acid-co-ε-caprolactone) 8:2 and 7:3 copolymers.

Mole Ratio of Copolymer*	Sample Condition	ΔH_c (J/g)	ΔH_f (J/g)	T_c** (°C)	T_m*** (°C)
8:2	before spinning	-	29.72	-	150.70
	after spinning	-20.53	27.05	83.23	150.00
	after annealing	-	29.54	-	151.85
7:3	before spinning	-	20.91	-	114.86
	after spinning	-	15.45	-	119.44
	after annealing	-	18.70	-	118.66

* L-lactide : ε-caprolactone

** crystallisation peak maximum temperature

*** melting peak maximum temperature

5.5.2 Thermogravimetry

5.5.2.1 Polypropylene

The TG thermogram of one of the polypropylene monofilaments is shown in Fig. 5.16 below.

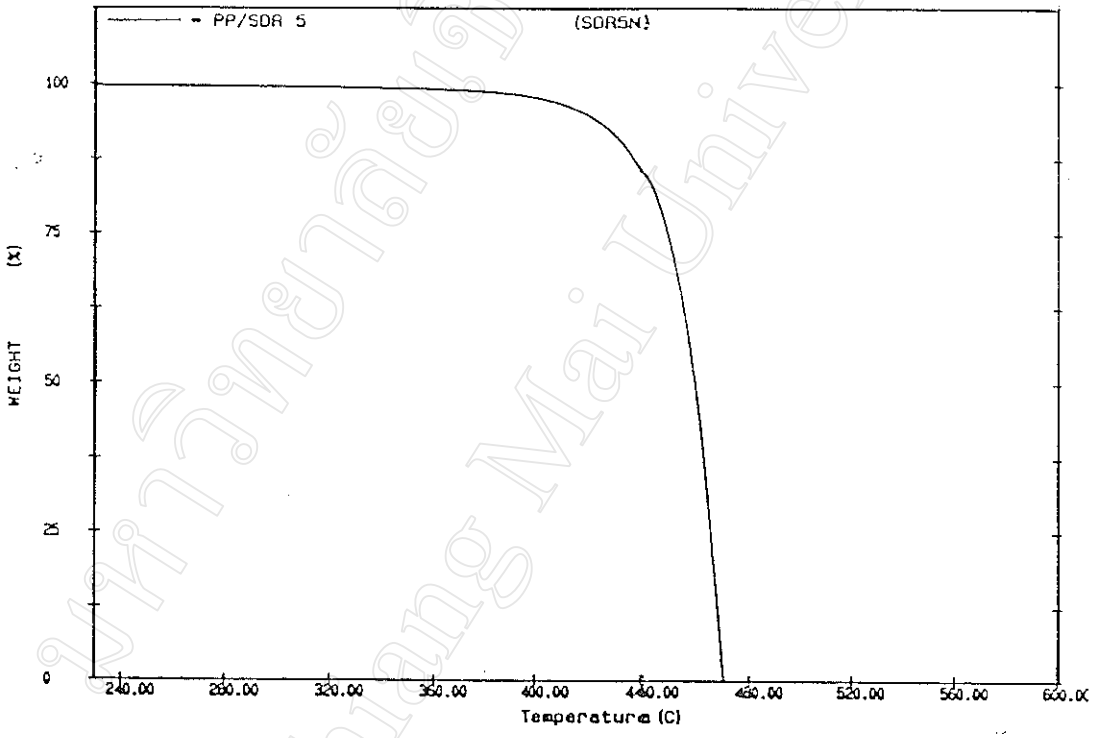

Fig. 5.16 TG thermogram of polypropylene monofilament (SDR 5) after melt spinning. (Heating rate = 20°C/min in N_2)

5.5.2.2 Poly(L-lactic acid-co-ε-caprolactone)

The TG thermograms of the poly(L-lactic acid-co-ε-caprolactone) 8:2 and 7:3 monofilaments are shown in Fig. 5.17 below.

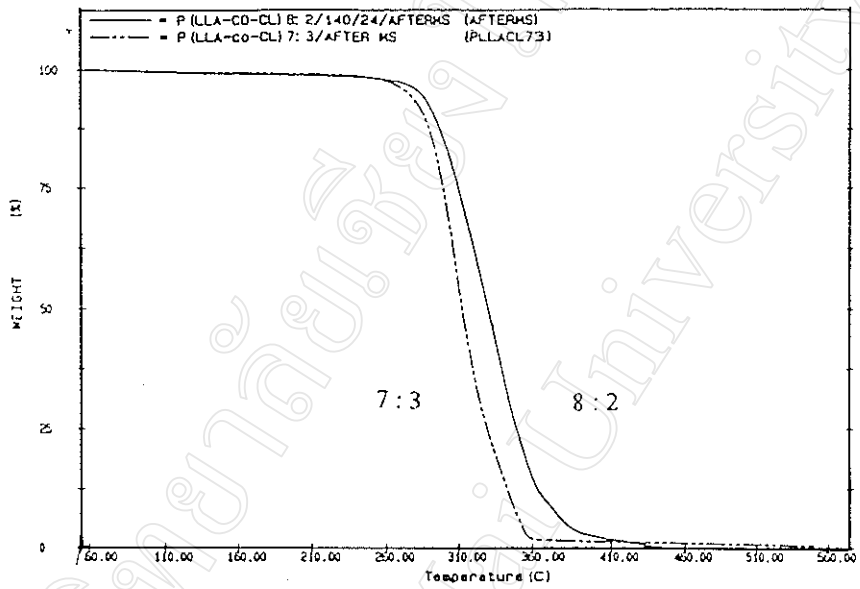

Fig. 5.17 TG thermograms of poly(L-lactic acid-co-ε-caprolactone) 8:2 and 7:3 monofilaments after melt spinning. (Heating rate = 20°C/min in N_2)

These TG thermograms, similar to those previously for before melt spinning, support the view that melt spinning of the polypropylene and poly(L-lactic-co-ε-caprolactone) samples has not caused any significant thermal degradation to occur. The TG thermograms after melt spinning look very similar to those before melt spinning (see section 5.1.2 previously). Also, there were no visible signs of any discoloration in any of the polymer samples after melt spinning. This processing stability is especially important in the case of the poly(L-lactic acid-co-ε-caprolactone) samples which are intended for use in surgical suture applications.

5.6 Microscopy

Some of the surface features of the polypropylene and poly(L-lactic acid-co-ε-caprolactone) monofilaments are shown in the photomicrographs in Figs. 5.18 and 5.19. The main features of interest are:

(a) the uniformity of filament diameter
(b) the surface texture (smoothness)
(c) the nature of any surface defects, if any

Examples of the types of surface defects which can occur during melt spinning (e.g., necking, void formation) are shown in Fig. 5.20.

(a)

Fig. 5.18 Photomicrographs of polypropylene monofiiaments (magnification x 10):

(a) spin-drawn only, SDR 7
(b) spin-drawn and off-line hot drawn, SDR 7 + OLDR 8

(b)

Fig. 5.18 Photomicrographs of polypropylene monofilaments (magnification x 10):

(a) spin-drawn only, SDR 7
(b) spin-drawn and off-line hot drawn, SDR 7 + OLDR 8

(a)

(b)

Fig. 5.19 Photomicrographs of poly(L-lactic acid-co-ε-caprolactone) melt spun (undrawn) monofilaments (magnification x 10):

(a) 7:3 copolymer
(b) 8:2 copolymer

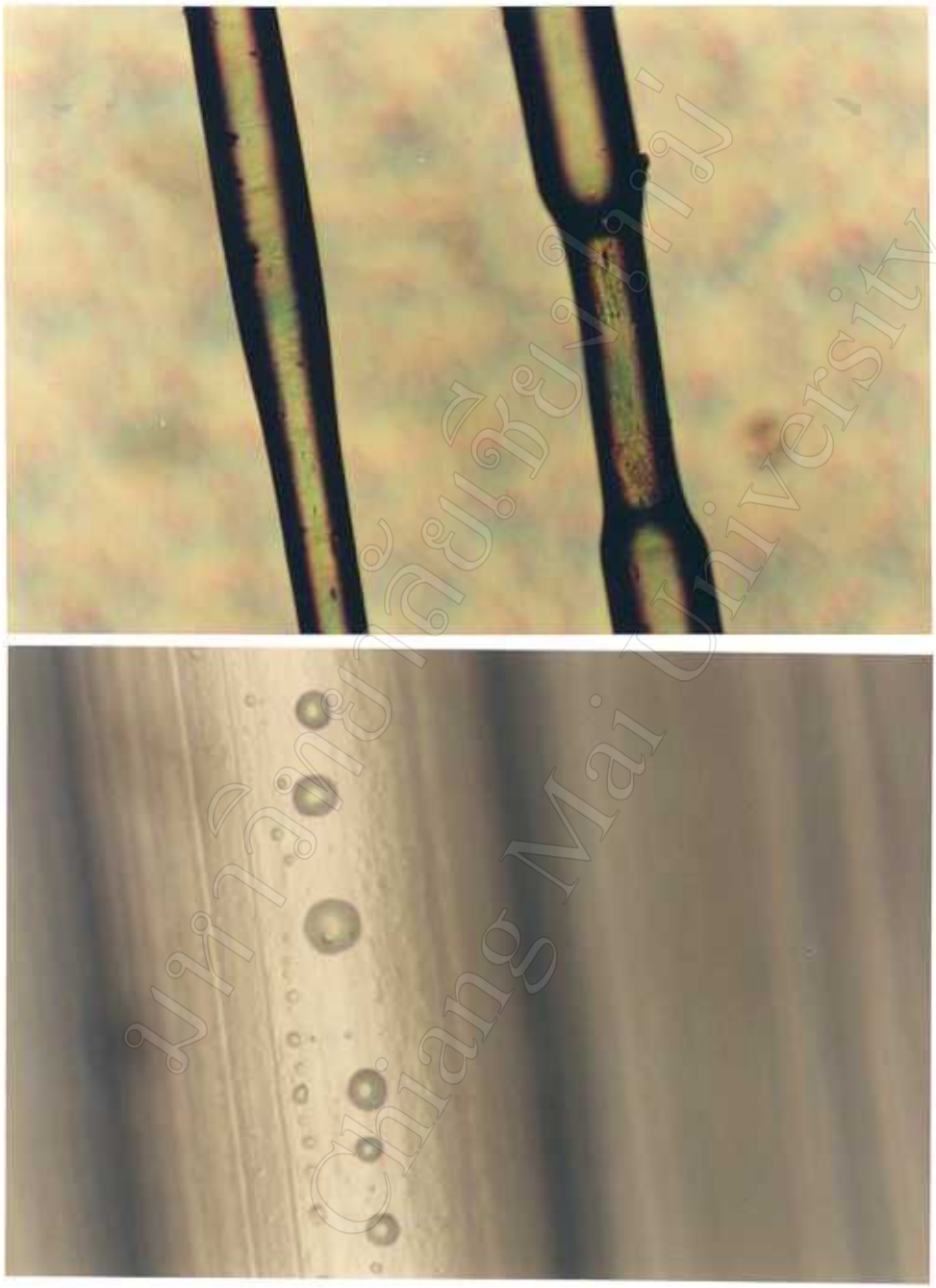

(a)

(b)

Fig. 5.20 Surface defects which can occur during melt spinning:

(a) necking
(b) microvoids

5.7 Linear Density

The units of linear density used for fibres are either 'denier' or 'tex'. The denier is defined as the mass in grams of 9000 meters of the material. An example of the calculation of linear density is shown below:

For the polypropylene monofilament, SDR 5

a length of 1 m has an average weight = 0.1362 g (from direct weighing)

therefore, a length of 9000 m has an average weight = $\frac{0.1362 \times 9000}{1}$ g

= 1226 denier

or, alternatively, since 1 denier = 0.1111 tex

linear density of the monofilament = 136 tex

Table 5.12 Linear densities of the spin-drawn polypropylene monofilaments.

SDR	Linear Density	
	denier	tex
5	1226	136
6	991	110
7	888	98.7
8	705	78.3
11	576	64.0
14	388	43.1
21	284	31.6
28	216	24.0
7(TCZ1)	870	96.7
7(TCZ2)	883	98.1
7(TCZ3)	858	95.3

5.8 Mechanical Properties

There are many mechanical properties that can be determined from mechanical tensile tests. The methods of calculation of some of these properties for one of the polypropylene monofilaments are shown below.

Sample Calculation:

For Sample No. 1 in Table 5.13 (see page 116)

from size measurement of the spin-drawn polypropylene monofilament SDR 5

diameter (d) = 0.43 mm (average of 5 readings)
radius (r) = 0.22 mm

Cross-sectional Area (A_o)

$$A_o = \pi r^2$$

$$= \pi(0.22 \text{ mm})^2$$

$$= 1.5 \times 10^{-7} \text{ m}^2$$

Cross-sectional Area at Break (A)

$$A_o l_o = Al$$

where A_o = initial cross-sectional area
l_o = gauge length
A = cross-sectional area at break
$l = l_o + \Delta l$ = extended length at break

Therefore, $$A = A_o\left(\frac{l_o}{l_o + \Delta l}\right)$$

$$= (1.5 \times 10^{-7}\ m^2)\left(\frac{30\ mm}{600.6\ mm}\right)$$

$$= 7.5 \times 10^{-9}\ m^2$$

Ultimate Tensile Strength at Break (Stress at Break), σ_B

ultimate tensile strength at break $= \frac{L_{max}}{A}$ (L_{max} = max. load at break)

$$= \frac{7.782\ N}{7.5 \times 10^{-9}\ m^2}$$

$$= 1038 \times 10^6\ N\ m^{-2}\ (Pa)$$

$$= 1038\ MPa$$

Breaking Tenacity

$$\text{breaking tenacity} = \frac{L_{max}\ (N)}{\text{Linear Density (tex)}}$$

From Table 5.13, the SDR 5 monofilament has a linear density of 136 tex

Therefore $$\text{breaking tenacity} = \frac{7.782\ N}{136\ tex}$$

$$= 5.72 \times 10^{-2}\ N\ tex^{-1}$$

Elongation at Break (Strain), ε_B

$$\text{elongation at break} = \frac{\text{increase in length}}{\text{initial length}} = \frac{\Delta l}{l_o} \times 100\%$$

$$= \frac{570.6}{30.00} \times 100\%$$

$$= 1902\%$$

Modulus of Elasticity or Young's Modulus (E)

$$E = \frac{\text{stress}}{\text{strain}} = \frac{L \times l_o}{A_o \times \Delta l}$$

$$= \frac{(\text{slope of the initial linear portion of the stress-strain curve}) \times l_o}{A_o}$$

$$= \frac{(4600\ \text{N m}^{-1})\ (30.0 \times 10^{-3}\ \text{m})}{1.5 \times 10^{-7}\ \text{m}^2}$$

$$= 920\ \text{MPa}$$

Examples of the stress-strain curves of the polypropylene monofilaments, commercial surgical sutures and synthesized poly(L-lactic acid-co-ε-caprolactone) monofilaments are shown in Figs. 5.21, 5.22 and 5.23 respectively. The construction of the initial linear portion of the stress-strain curve used in the above calculation is shown in Fig. 5.21 on the following page.

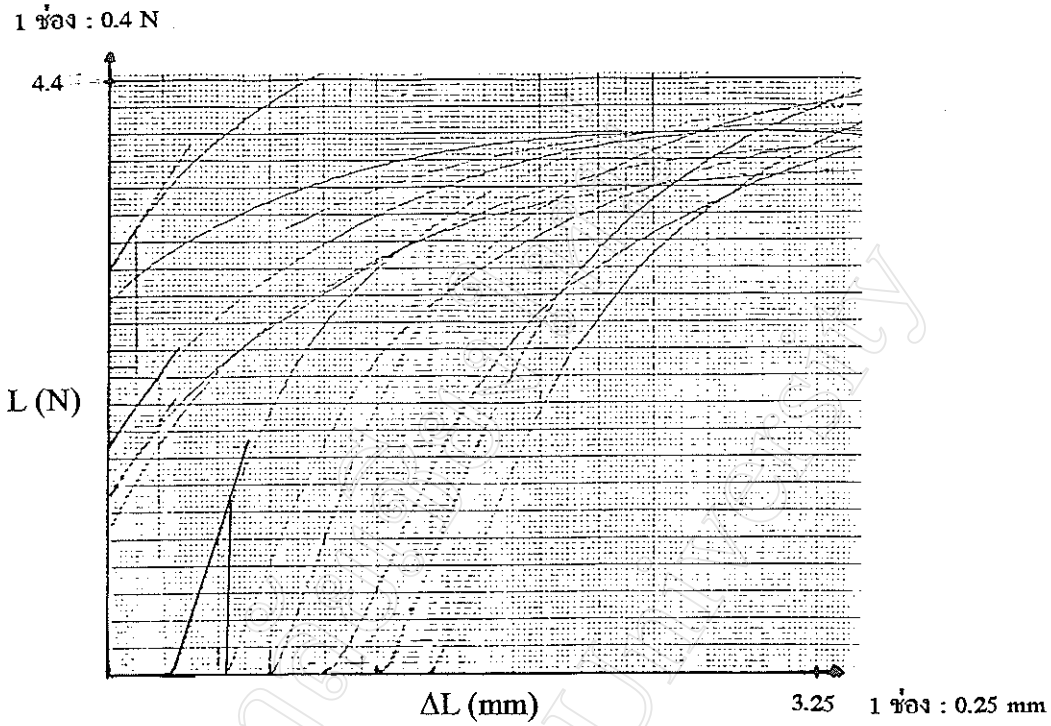

Fig. 5.21 Stress-strain curves for the polypropylene monofilament SDR 5 (sample No. 1 in Table 5.13) showing the initial linear slope used for calculating the modulus of elasticity (Young's Modulus).

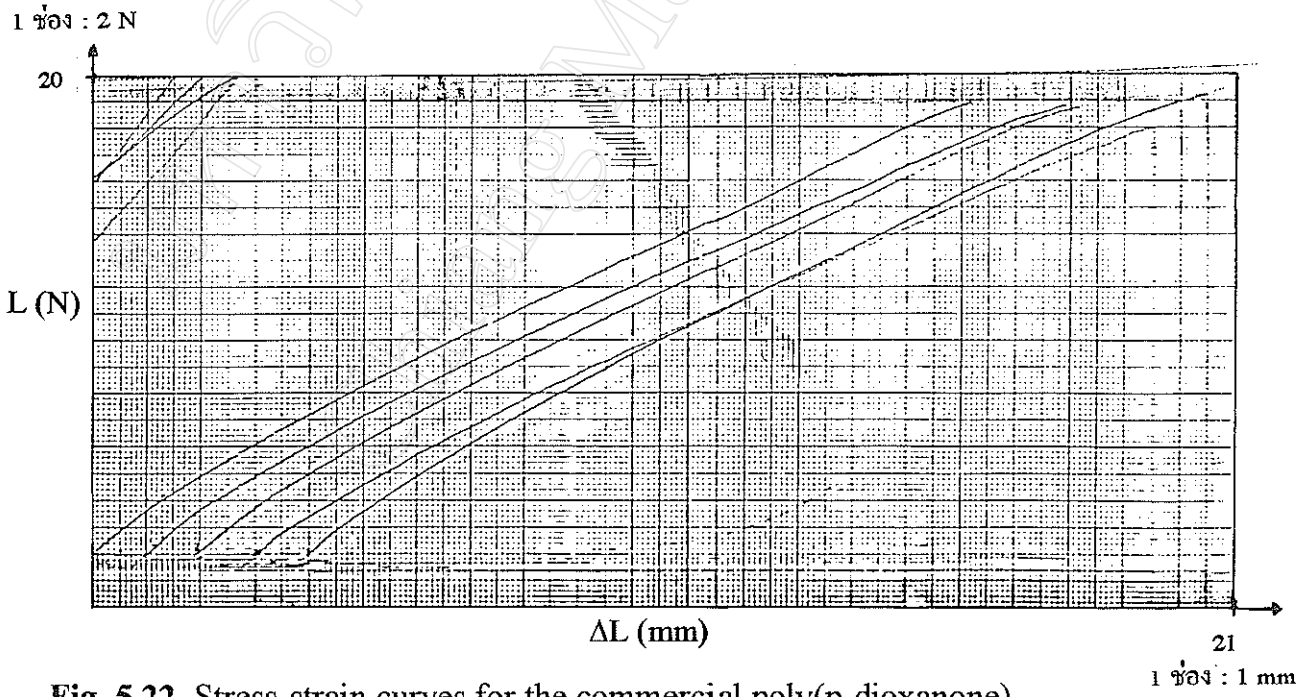

Fig. 5.22 Stress-strain curves for the commercial poly(p-dioxanone) (PDS II 4-0) monofilament suture.

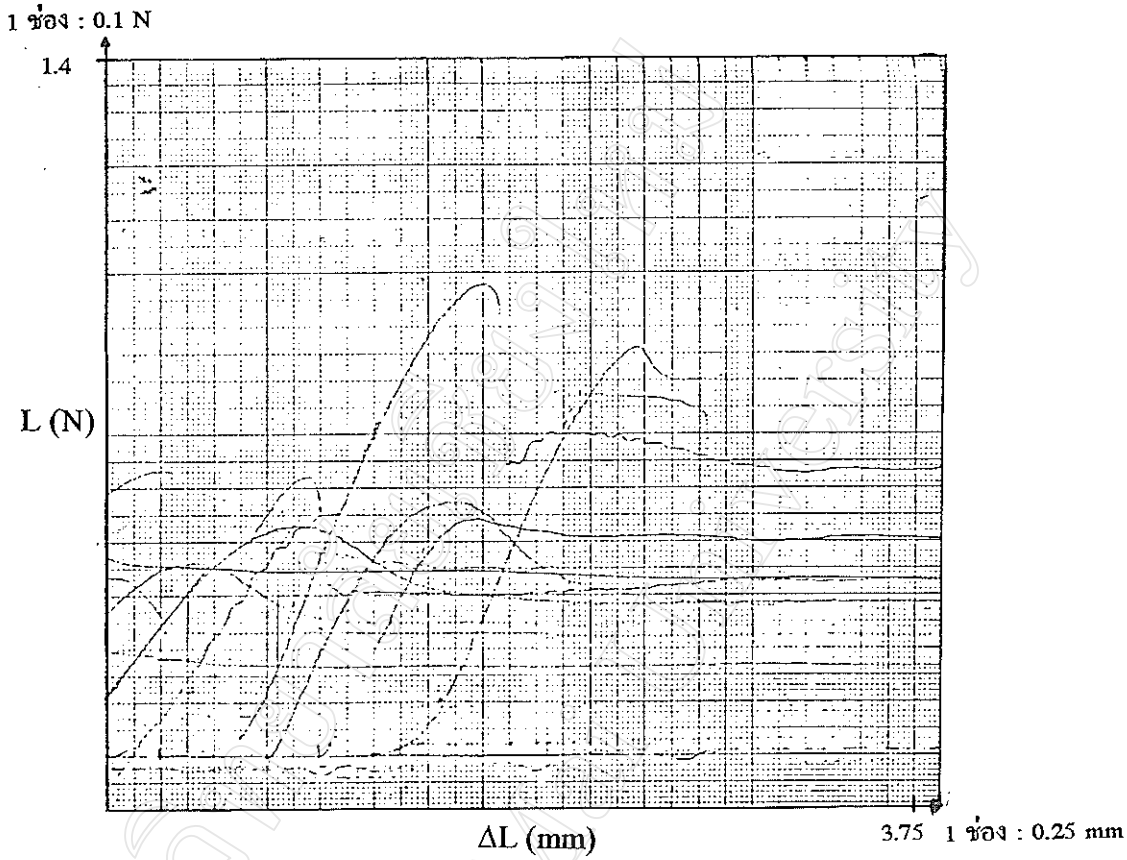

Fig. 5.23 Stress-strain curves for the synthesized poly(L-lactic acid-co-ε-caprolactone) 8:2 monofilaments.

For convenience in locating the mechanical test results in this thesis for the polypropylene monofilaments, commercial surgical sutures and synthesized poly(L-lactic acid-co-ε-caprolactone) monofilaments, the various tables are indexed on the following pages 114-115.

TABLE INDEX

TABLE INDEX (continued)

Table 5.13 Mechanical property test results for the polypropylene monofilament SDR 5.

Average Linear Density = 136 tex [a]

Sample No.	Avg. Diameter [b] (± 0.01 mm)	$A_o \times 10^7$ (m^2)	$A \times 10^9$ (m^2)	L_{max} (N)	σ_B [c] (MPa)
1	0.43	1.5	7.5	7.782	1038
2	0.42	1.4	6.8	7.683	1130
3	0.40	1.2	6.8	6.684	983
4	0.41	1.2	6.2	7.299	1177
5	0.42	1.4	6.5	7.992	1219

Sample No.	l_o (mm)	Δl_{max} (mm)	Strain (ε_B) (%) [d]
1	30.0	570.6	1902
2	30.0	589.6	1965
3	30.0	495.1	1650
4	30.0	551.8	1839
5	30.0	611.5	2038

Sample No.	σ_B (MPa)	Tenacity $\times 10^2$ (N/tex)	ε_B (%)	Slope [e] L/Δl (N/m)	Young's Modulus (MPa)
1	1038	5.72	1902	4600	920
2	1130	5.65	1965	4200	900
3	983	4.91	1650	2800	700
4	1177	5.37	1839	4100	1025
5	1219	5.88	2038	4053	868
Avg.	1089	5.51	1879	-	883

[a] average of 3 determinations
[b] average of 5 readings taken using a micrometer
[c] maximum stress (or ultimate tensile strength) at break
[d] maximum strain (or elongation) at break
[e] initial slope of the stress-strain curve

Table 5.14 Mechanical property test results for the polypropylene monofilament SDR 7.

Average Linear Density = 98.7 tex

Sample No.	Avg. Diameter (± 0.01 mm)	$A_o \times 10^7$ (m^2)	$A \times 10^9$ (m^2)	L_{max} (N)	σ_B (MPa)
1	0.34	0.91	6.1	4.851	795
2	0.39	1.2	7.5	6.376	850
3	0.38	1.1	5.5	6.325	1150
4	0.37	1.0	4.9	6.268	1279
5	0.35	1.0	5.4	5.396	999

Sample No.	l_o (mm)	Δl_{max} (mm)	Strain (ε_B) (%)
1	30.0	417.7	1392
2	30.0	447.4	1491
3	30.0	566.1	1887
4	30.0	576.1	1920
5	30.0	521.8	1739

Sample No.	σ_B (MPa)	Tenacity $\times 10^2$ (N/tex)	ε_B (%)	Slope ($L/\Delta l$) (N/m)	Young's Modulus (MPa)
1	795	4.91	1392	2666	879
2	850	6.46	1491	3636	909
3	1150	6.41	1887	3200	872
4	1279	6.35	1920	3040	912
5	999	5.47	1739	2954	923
Avg.	1015	5.92	1686	-	899

Table 5.15 Mechanical property test results for the polypropylene monofilament SDR 11.

Average Linear Density = 64.0 tex

Sample No.	Avg. Diameter (± 0.01 mm)	$A_o \times 10^7$ (m^2)	$A \times 10^9$ (m^2)	L_{max} (N)	σ_B (MPa)
1	0.29	0.62	3.5	4.172	1192
2	0.27	0.62	3.5	3.468	991
3	0.30	0.70	3.6	3.925	1090
4	0.28	0.62	3.8	3.844	1012
5	0.30	0.71	4.3	4.123	959

Sample No.	l_o (mm)	Δl_{max} (mm)	Strain (ε_B) (%)
1	30.0	503.5	1678
2	30.0	496.3	1654
3	30.0	560.6	1867
4	30.0	453.4	1511
5	30.0	461.3	1538

Sample No.	σ_B (MPa)	Tenacity $\times 10^2$ (N/tex)	ε_B (%)	Slope (L/Δl) (N/m)	Young's Modulus (MPa)
1	1192	6.52	1678	2200	1064
2	991	5.42	1654	1867	903
3	1090	6.13	1867	1778	762
4	1012	6.00	1511	2036	985
5	959	6.44	1538	2133	901
Avg.	1049	6.10	1650	-	923

Table 5.16 Mechanical property test results for the polypropylene monofilament SDR 14.

Average Linear Density = 43.1 tex

Sample No.	Avg. Diameter (± 0.01 mm)	$A_o \times 10^8$ (m^2)	$A \times 10^9$ (m^2)	L_{max} (N)	σ_B (MPa)
1	0.24	4.5	2.8	2.977	1063
2	0.24	4.5	2.8	2.950	1053
3	0.24	4.5	2.7	3.028	1121
4	0.27	6.2	4.9	3.366	687
5	0.24	4.5	4.0	2.714	678

Sample No.	l_o (mm)	Δl_{max} (mm)	Strain (ε_B) (%)
1	30.0	459.2	1521
2	30.0	442.9	1476
3	30.0	465.9	1552
4	30.0	345.9	1153
5	30.0	305.2	1017

Sample No.	σ_B (MPa)	Tenacity $\times 10^2$ (N/tex)	ε_B (%)	Slope $L/\Delta l$ (N/m)	Young's Modulus (MPa)
1	1063	6.91	1521	1467	978
2	1053	6.84	1476	1600	1067
3	1121	7.03	1552	1867	1244
4	687	7.81	1153	1846	893
5	678	6.30	1017	1354	902
Avg.	920	6.98	1344	-	1017

Table 5.17 Mechanical property test results for the polypropylene monofilament SDR 21.

Average Linear Density = 31.6 tex

Sample No.	Avg. Diameter (± 0.01 mm)	$A_o \times 10^8$ (m^2)	$A \times 10^9$ (m^2)	L_{max} (N)	σ_B (MPa)
1	0.22	3.8	2.6	2.529	973
2	0.21	3.1	2.6	2.293	882
3	0.23	4.5	3.0	2.596	865
4	0.21	3.1	2.3	2.290	996
5	0.19	3.1	2.6	2.046	787

Sample No.	l_o (mm)	Δl_{max} (mm)	Strain (ε_B) (%)
1	30.0	412.6	1375
2	30.0	334.7	1116
3	30.0	414.9	1383
4	30.0	380.5	1268
5	30.0	329.7	1099

Sample No.	σ_B (MPa)	Tenacity $\times 10^2$ (N/d)	ε_B (%)	Slope (L/Δl) (N/m)	Young's Modulus (MPa)
1	973	8.00	1375	1387	1095
2	882	7.26	1116	889	860
3	865	8.22	1383	1511	1007
4	996	7.25	1268	1200	1161
5	787	6.47	1099	800	774
Avg.	901	7.44	1248	-	984

Table 5.18 Mechanical property test results for the polypropylene monofilament SDR 28.

Average Linear Density = 24.0 tex

Sample No.	Avg. Diameter (± 0.01 mm)	$A_o \times 10^8$ (m^2)	$A \times 10^9$ (m^2)	L_{max} (N)	σ_B (MPa)
1	0.18	2.5	1.9	2.051	1079
2	0.19	2.8	2.2	2.040	927
3	0.19	2.8	2.0	2.056	1028
4	0.19	2.8	2.3	1.981	861
5	0.19	2.8	2.2	1.946	884

Sample No.	l_o (mm)	Δl_{max} (mm)	Strain (ε_B) (%)
1	30.0	355.9	1186
2	30.0	354.6	1180
3	30.0	379.6	1265
4	30.0	337.5	1125
5	30.0	355.9	1186

Sample No.	σ_B (MPa)	Tenacity $\times 10^2$ (N/tex)	ε_B (%)	Slope (L/Δl) (N/m)	Young's Modulus (MPa)
1	1079	8.54	1186	985	1182
2	927	8.50	1180	1382	1337
3	1028	8.57	1256	1091	1056
4	861	8.25	1125	1382	1337
5	884	8.11	1186	1067	1032
Avg.	956	8.39	1188	1181	1189

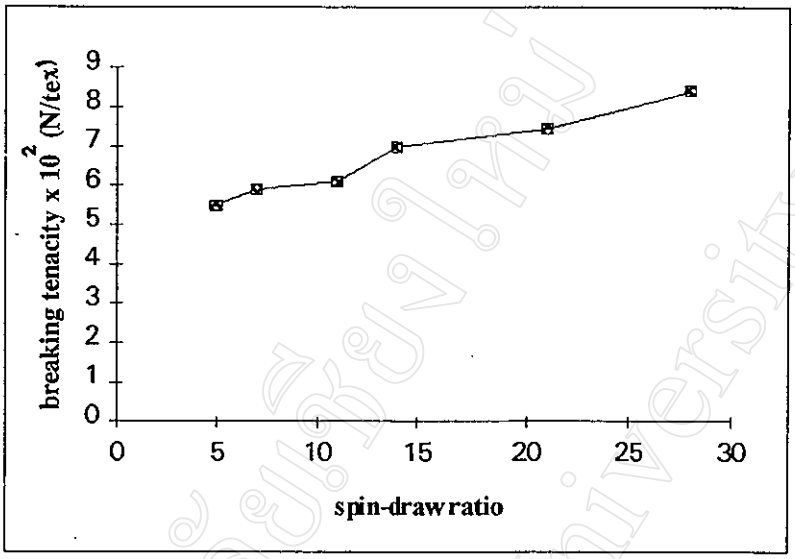

Fig. 5.24 Breaking tenacity of the polypropylene monofilaments as a function of spin-draw ratio.

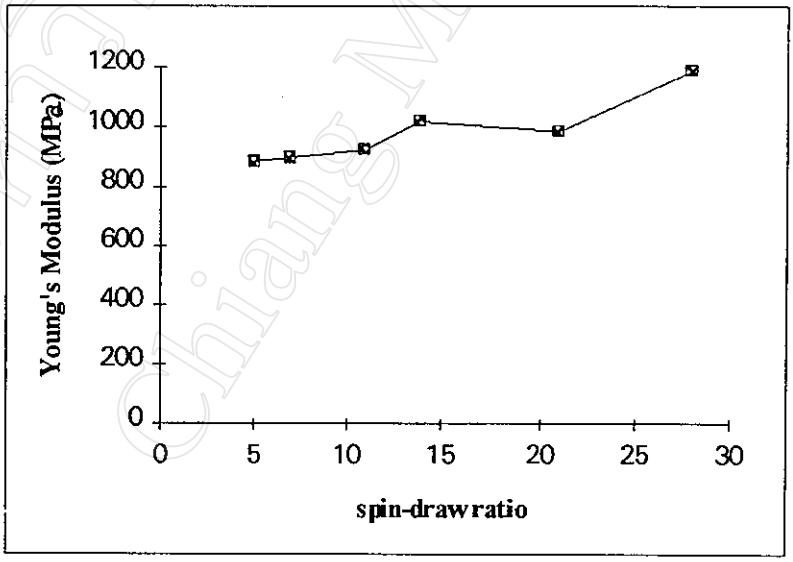

Fig. 5.25 Young's modulus of the polypropylene monofilaments as a function of spin-draw ratio.

Table 5.19 Mechanical property test results for the polypropylene monofilament SDR 7, TCZ1.

Average Linear Density = 96.7 tex

Sample No.	Avg. Diameter (± 0.01 mm)	$A_o \times 10^7$ (m^2)	$A \times 10^9$ (m^2)	L_{max} (N)	σ_B (MPa)
1	0.38	1.1	5.8	6.827	1117
2	0.38	1.1	5.9	6.953	1178
3	0.35	1.0	5.2	5.957	1146
4	0.36	1.0	5.3	6.266	1182
5	0.36	1.0	5.5	6.577	1196

Sample No.	l_o (mm)	Δl_{max} (mm)	Strain (ε_B) (%)
1	30.0	534.4	1781
2	30.0	533.0	1777
3	30.0	547.3	1791
4	30.0	537.2	1728
5	30.0	518.5	1780

Sample No.	σ_B (MPa)	Tenacity $\times 10^2$ (N/tex)	ε_B (%)	Slope (L/Δl) (N/m)	Young's Modulus (MPa)
1	1177	7.06	1781	2720	741
2	1178	7.19	1777	2400	654
3	1146	6.16	1791	2308	692
4	1182	6.48	1728	2844	853
5	1196	6.80	1780	2353	706
Avg.	1176	6.74	1771	-	729

Table 5.20 Mechanical property test results for the polypropylene monofilament SDR 7, TCZ2.

Average Linear Density = 98.0 tex

Sample No.	Avg. Diameter (± 0.01 mm)	$A_o \times 10^7$ (m^2)	$A \times 10^9$ (m^2)	L_{max} (N)	σ_B (MPa)
1	0.39	1.2	6.2	7.361	1187
2	0.38	1.1	5.0	7.068	1414
3	0.37	1.0	4.9	6.768	1381
4	0.36	1.0	5.3	6.365	1201
5	0.37	1.0	5.1	6.711	1342

Sample No.	l_o (mm)	Δl_{max} (mm)	Strain (ε_B) (%)
1	30.0	548.7	1829
2	30.0	628.7	2096
3	30.0	580.1	1934
4	30.0	532.9	1776
5	30.0	559.6	1865

Sample No.	σ_B (MPa)	Tenacity $\times 10^2$ (N/tex)	ε_B (%)	Slope ($L/\Delta l$) (N/m)	Young's Modulus (MPa)
1	1187	7.51	1829	3093	773
2	1414	7.21	2096	3200	873
3	1381	6.91	1934	2779	834
4	1201	6.49	1176	2189	657
5	1342	6.85	1865	2880	864
Avg.	1305	6.99	1900	-	800

Table 5.21 Mechanical property test results for the polypropylene monofilament SDR 7, TCZ3.

Average Linear Density = 95.3 tex

Sample No.	Avg. Diameter (± 0.01 mm)	$A_o \times 10^7$ $(m)^2$	$A \times 10^9$ $(m)^2$	L_{max} (N)	σ_B (MPa)
1	0.37	1.0	5.2	6.744	1297
2	0.36	1.0	6.0	6.395	1066
3	0.38	1.1	5.8	7.087	1222
4	0.37	1.0	5.2	6.489	1248
5	0.36	1.0	6.4	6.145	960

Sample No.	l_o (mm)	Δl_{max} (mm)	Strain (ε_B) (%)
1	30.0	549.9	1833
2	30.0	463.0	1543
3	30.0	537.9	1793
4	30.0	551.0	1837
5	30.0	437.2	1693

Sample No.	σ_B (MPa)	Tenacity $\times 10^2$ (N/tex)	ε_B (%)	Slope (L/Δl) (N/m)	Young's Modulus (MPa)
1	1297	7.08	1833	3000	900
2	1066	6.51	1543	2824	847
3	1222	7.44	1793	3345	912
4	1248	6.81	1837	3022	907
5	960	6.45	1693	2259	678
Avg.	1159	6.86	1740	-	849

Similarly, the spin-drawn/off-line hot drawn polypropylene monofilaments were also tested to determine their mechanical properties. Their mechanical property test results are shown in Tables 5.22 - 5.30.

Table 5.22 Mechanical property test results for the polypropylene monofilament SDR 5, OLDR 8 and T_{OLHD} = 120°C.

Sample No.	Avg. Diameter (± 0.01 mm)	$A_o \times 10^8$ (m^2)	$A \times 10^8$ (m^2)	L_{max} (N)	σ_B (MPa)
1	0.13	1.3	1.1	7.412	674
2	0.14	1.5	1.3	8.352	642
3	0.14	1.5	1.2	8.765	730
4	0.14	1.5	1.2	9.168	764
5	0.14	1.5	1.3	7.216	555

Sample No.	l_o (mm)	Δl_{max} (mm)	Strain (ε_B) (%)
1	30.0	4.060	14.0
2	30.0	4.800	16.0
3	30.0	9.110	30.0
4	30.0	5.860	20.0
5	30.0	4.110	14.0

Sample No.	σ_B (MPa)	ε_B (%)	Slope (L/Δl) (N/m)	Young's Modulus (MPa)
1	674	14.0	3200	7385
2	642	16.0	3520	7040
3	730	30.0	2800	5600
4	764	20.0	2756	6200
5	555	14.0	3600	7200
Avg.	673	19.0	-	6685

Table 5.23 Mechanical property test results for the polypropylene monofilament SDR 7, OLDR 8 and T_{OLHD} = 120°C

Sample No.	Avg. Diameter (± 0.01 mm)	A_o x 10^8 $(m)^2$	A x 10Û¥- $(m)^2$	L_{max} (N)	σ_B (MPa)
1	0.12	1.1	7.4	6.571	888
2	0.12	1.1	8.9	7.482	841
3	0.13	1.3	11	7.001	636
4	0.13	1.3	10	7.952	795
5	0.12	1.1	9.4	6.317	672

Sample No.	l_o (mm)	Δl_{max} (mm)	Strain (ε_B) (%)
1	30.0	14.81	49.0
2	30.0	6.990	23.0
3	30.0	5.990	20.0
4	30.0	8.180	27.0
5	30.0	5.160	17.0

Sample No.	σ_B (MPa)	ε_B (%)	Slope (L/Δl) (N/m)	Young's Modulus (MPa)
1	888	49.0	2200	6000
2	841	23.0	2514	6857
3	636	20.0	2267	5231
4	795	27.0	2109	4867
5	672	17.0	2000	5454
Avg.	766	27.0	-	5682

Table 5.24 Mechanical property test results for the polypropylene monofilament SDR 11, OLDR 8 and T_{OLHD} = 120°C.

Sample No.	Avg. Diameter (± 0.01 mm)	$A_o \times 10^8$ (m^2)	$A \times 10^8$ (m^2)	L_{max} (N)	σ_B (MPa)
1	0.14	1.5	1.1	5.546	504
2	0.13	1.3	0.97	5.259	542
3	0.13	1.3	1.0	5.568	557
4	0.14	1.5	1.0	5.530	503
5	0.15	1.8	1.4	5.483	392

Sample No.	l_o (mm)	Δl_{max} (mm)	Strain (ε_B) (%)
1	30.0	9.920	33.00
2	30.0	10.16	29.00
3	30.0	8.830	35.00
4	30.0	10.42	33.00
5	30.0	9.840	33.00

Sample No.	σ_B (MPa)	ε_B (%)	Slope (L/Δl) (N/m)	Young's Modulus (MPa)
1	504	33.0	2267	4533
2	542	29.0	1600	3692
3	557	35.0	2080	4800
4	503	33.0	3400	6800
5	392	33.0	1600	2667
Avg.	500	33.0	-	4498

Table 5.25 Mechanical property test results for the polypropylene monofilament SDR 14, OLDR 8 and T_{OLHD} = 120°C.

Sample No.	Avg. Diameter (±0.01 mm)	$A_o \times 10^8$ (m^2)	$A \times 10^9$ (m^2)	L_{max} (N)	σ_B (MPa)
1	0.12	1.1	8.4	4.482	534
2	0.11	0.95	6.8	3.427	504
3	0.13	1.3	10	3.544	354
4	0.12	1.1	8.5	4.475	526
5	0.11	0.95	7.0	3.389	484

Sample No.	l_o (mm)	Δl_{max} (mm)	Strain (ε_B) (%)
1	30.0	9.070	30.0
2	30.0	11.85	40.0
3	30.0	8.390	28.0
4	30.0	8.820	29.0
5	30.0	10.97	36.0

Sample No.	σ_B (MPa)	ε_B (%)	Slope ($L/\Delta l$) (N/m)	Young's Modulus (MPa)
1	534	30.0	1257	3428
2	504	40.0	1028	3248
3	354	28.0	1227	2831
4	526	29.0	1333	3636
5	484	36.0	1133	3579
Avg.	480	33.0	-	3344

Table 5.26 Mechanical property test results for the polypropylene monofilament SDR 21, OLDR 8 and T_{OLHD} = 120°C.

Sample No.	Avg. Diameter (± 0.01 mm)	$A_o \times 10^9$ (m^2)	$A \times 10^9$ (m^2)	L_{max} (N)	σ_B (MPa)
1	0.08	5.0	4.1	2.817	687
2	0.08	5.0	4.2	2.772	660
3	0.08	5.0	4.2	2.772	660
4	0.08	5.0	4.1	2.748	670
5	0.08	5.0	4.3	2.341	544

Sample No.	l_o (mm)	Δl_{max} (mm)	Strain (ε_B) (%)
1	30.0	6.570	22.0
2	30.0	5.810	19.0
3	30.0	5.800	19.0
4	30.0	6.970	23.0
5	30.0	5.070	17.0

Sample No.	σ_B (MPa)	ε_B (%)	Slope (L/Δl) (N/m)	Young's Modulus (MPa)
1	687	22.0	800	4781
2	660	19.0	914	5464
3	660	19.0	914	5464
4	670	23.0	800	4781
5	544	17.0	800	4781
Avg.	644	20.0	-	5055

Table 5.27 Mechanical property test results for the polypropylene monofilament SDR 28, OLDR 8 and T_{OLHD} = 120°C.

Sample No.	Avg. Diameter (± 0.01 mm)	$A_o \times 10^9$ (m^2)	$A \times 10^9$ (m^2)	L_{max} (N)	σ_B (MPa)
1	0.08	5.0	3.6	2.271	631
2	0.08	5.0	4.1	2.263	552
3	0.07	3.8	3.0	2.012	671
4	0.07	3.8	3.3	1.862	564
5	0.07	3.8	2.9	2.052	708

Sample No.	l_o (mm)	Δl_{max} (mm)	Strain (ε_B) (%)
1	30.0	7.650	26.0
2	30.0	6.620	22.0
3	30.0	8.570	28.0
4	30.0	4.750	16.0
5	30.0	8.670	29.0

Sample No.	σ_B (MPa)	ε_B (%)	Slope ($L/\Delta l$) (N/m)	Young's Modulus (MPa)
1	631	26.0	933	6222
2	552	22.0	686	4114
3	671	28.0	500	3658
4	564	16.0	800	5581
5	708	29.0	667	5263
Avg.	625	24.0	-	4968

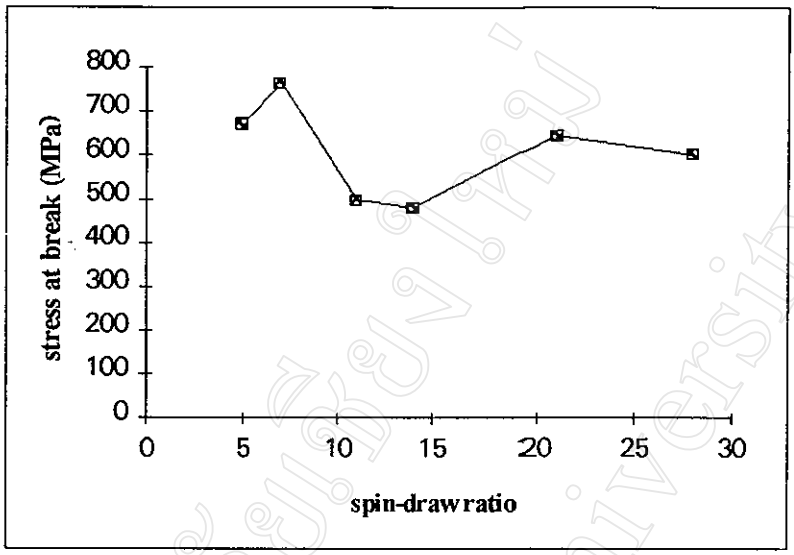

Fig. 5.26 Stress at break of the polypropylene monofilaments as a function of spin-draw ratio at OLDR 8 and T_{OLHD} = 120°C.

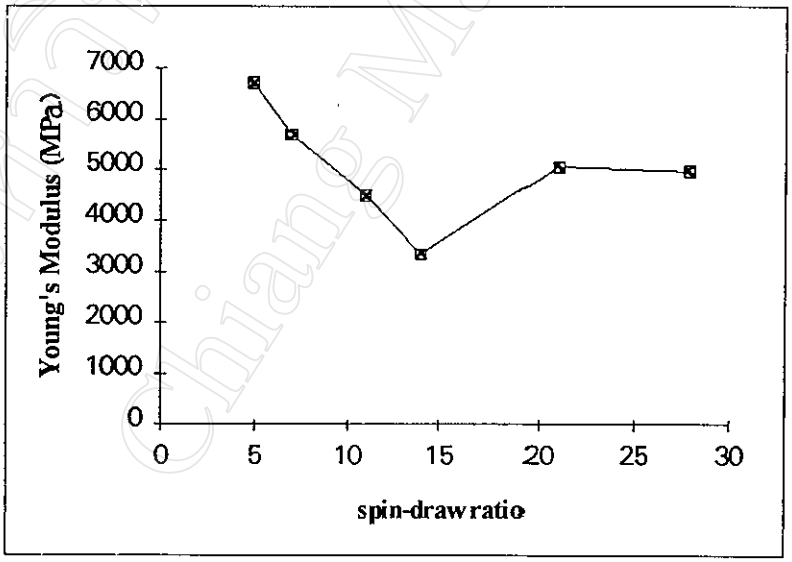

Fig. 5.27 Young's modulus of the polypropylene monofilaments as a function of spin-draw ratio at OLDR 8 and T_{OLHD} = 120°C.

Table 5.28 Mechanical property test results for the polypropylene monofilament SDR 7, OLDR 8, TCZ1 and T_{OLHD} = 120°C.

Sample No.	Avg. Diameter (± 0.01 mm)	$A_o \times 10^8$ (m^2)	$A \times 10^8$ (m^2)	L_{max} (N)	σ_B (MPa)
1	0.13	1.3	1.1	7.071	643
2	0.12	1.1	0.95	6.276	661
3	0.12	1.1	0.92	6.454	702
4	0.13	1.3	1.1	6.454	587
5	0.12	1.1	0.95	6.333	667

Sample No.	l_o (mm)	Δl_{max} (mm)	Strain (ε_B) (%)
1	30.0	5.370	18.0
2	30.0	4.820	16.0
3	30.0	5.920	20.0
4	30.0	5.360	18.0
5	30.0	4.760	16.0

Sample No.	σ_B (MPa)	ε_B (%)	Slope (L/Δl) (N/m)	Young's Modulus (MPa)
1	643	18.0	2667	6154
2	661	16.0	2400	6545
3	702	20.0	1600	4364
4	587	18.0	2400	5538
5	667	16.0	1840	5018
Avg.	652	18.0	-	5524

Table 5.29 Mechanical property test results for the polypropylene monofilament SDR 7, OLDR 8, TCZ2 and T_{OLHD} = 120°C.

Sample No.	Avg. Diameter (± 0.01 mm)	$A_o \times 10^8$ (m^2)	$A \times 10^8$ (m^2)	L_{max} (N)	σ_B (MPa)
1	0.15	1.8	1.0	7.895	790
2	0.13	1.3	1.1	7.036	640
3	0.14	1.5	1.2	7.350	612
4	0.15	1.8	1.4	7.968	569
5	0.15	1.8	1.4	7.984	570

Sample No.	l_o (mm)	Δl_{max} (mm)	Strain (ε_B) (%)
1	30.0	9.100	30.0
2	30.0	6.210	21.0.
3	30.0	8.960	30.0
4	30.0	8.960	30.0
5	30.0	8.450	28.0

Sample No.	σ_B (MPa)	ε_B (%)	Slope (L/Δl) (N/m)	Young's Modulus (MPa)
1	790	30.0	2628	4381
2	640	21.0	2667	6154
3	612	30.0	2533	5067
4	569	30.0	2533	4222
5	570	28.0	3400	5667
Avg.	636	28.0	-	5098

Table 5.30 Mechanical property test results for the polypropylene monofilament SDR 7, OLDR 8, TCZ3 and T_{OLHD} = 120°C.

Sample No.	Avg. Diameter (± 0.01 mm)	$A_o \times 10^8$ (m^2)	$A \times 10^8$ (m^2)	L_{max} (N)	σ_B (MPa)
1	0.13	1.3	1.1	8.110	737
2	0.13	1.3	1.1	7.874	716
3	0.14	1.5	1.2	8.392	699
4	0.13	1.3	1.1	7.388	672
5	0.13	1.3	1.1	7.587	690

Sample No.	l_o (mm)	Δl_{max} (mm)	Strain (ε_B) (%)
1	30.0	6.870	23.0
2	30.0	6.350	21.0
3	30.0	6.940	23.0
4	30.0	5.520	18.0
5	30.0	6.470	22.0

Sample No.	σ_B (MPa)	ε_B (%)	Slope (L/Δl) (N/m)	Young's Modulus (MPa)
1	737	23.0	2171	5011
2	716	21.0	2720	6277
3	699	23.0	2971	5943
4	672	18.0	2500	5769
5	690	22.0	2171	5011
Avg.	703	21.0	-	5602

The polypropylene monofilaments at four different off-line draw ratios: OLDR 2, 4, 6 and 8, and at three different OLHD temperatures: 100°C, 110°C and 120°C, were tested and their mechanical property test results are as shown in Tables 5.31 - 5.42.

Table 5.31 Mechanical property test results for the polypropylene monofilament SDR 7, OLDR 2 and T_{OLHD} = 100°C.

Sample No.	Avg. Diameter (± 0.01 mm)	$A_o \times 10^8$ (m^2)	$A \times 10^9$ (m^2)	L_{max} (N)	σ_B (MPa)
1	0.16	2.0	1.4	8.000	571
2	0.17	2.3	1.7	8.016	472
3	0.17	2.3	1.1	6.988	635
4	0.18	2.5	1.3	7.173	552
5	0.17	2.3	1.8	8.572	476

Sample No.	l_o (mm)	Δl_{max} (mm)	Strain (ε_B) (%)
1	30.0	40.00	40.0
2	30.0	37.00	37.0
3	30.0	100.0	100
4	30.0	94.00	94.0
5	30.0	28.00	28.0

Sample No.	σ_B (MPa)	ε_B (%)	Slope (L/Δl) (N/m)	Young's Modulus (MPa)
1	571	40.0	2711	4067
2	472	37.0	2954	3853
3	635	100	2254	2941
4	552	94.0	2720	3264
5	476	28.0	3378	4406
Avg.	541	60.0	-	3706

Table 5.32 Mechanical property test results for the polypropylene monofilament SDR 7, OLDR 4 and T_{OLHD} = 100°C.

Sample No.	Avg. Diameter (± 0.01 mm)	$A_o \times 10^8$ (m^2)	$A \times 10^8$ (m^2)	L_{max} (N)	σ_B (MPa)
1	0.18	2.5	2.2	7.681	349
2	0.18	2.5	1.9	7.976	420
3	0.18	2.5	1.4	7.852	561
4	0.18	2.5	1.4	7.635	545
5	0.18	2.5	1.8	8.188	455

Sample No.	l_o (mm)	Δl_{max} (mm)	Strain (ε_B) (%)
1	30.0	14.65	49.0
2	30.0	10.00	33.0
3	30.0	24.26	81.0
4	30.0	25.22	84.0
5	30.0	12.54	42.0

Sample No.	σ_B (MPa)	ε_B (%)	Slope (L/Δl) (N/m)	Young's Modulus (MPa)
1	349	19.0	2667	3200
2	420	33.0	2541	3049
3	561	81.0	3289	3947
4	545	84.0	2764	3316
5	455	42.0	3200	3840
Avg.	466	58.0	-	3470

Table 5.33 Mechanical property test results for the polypropylene monofilament SDR 7, OLDR 6 and T_{OLHD} = 100°C.

Sample No.	Avg. Diameter (± 0.01 mm)	$A_o \times 10^8$ (m^2)	$A \times 10^8$ (m^2)	L_{max} (N)	σ_B (MPa)
1	0.17	2.3	1.8	8.397	466
2	0.16	2.0	1.6	8.631	539
3	0.16	2.0	1.5	8.427	562
4	0.16	2.0	1.5	8.368	558
5	0.15	1.8	1.4	8.314	594

Sample No.	l_o (mm)	Δl_{max} (mm)	Strain (ε_B) (%)
1	30.0	8.900	30.0
2	30.0	7.790	26.0
3	30.0	8.954	30.0
4	30.0	9.020	32.0
5	30.0	9.450	30.0

Sample No.	σ_B (MPa)	ε_B (%)	Slope (L/Δl) (N/m)	Young's Modulus (MPa)
1	466	30.0	2000	2609
2	539	26.0	2215	3231
3	562	30.0	2700	4050
4	558	30.0	3040	4560
5	594	32.0	2494	4157
Avg.	544	30.0	-	3721

Table 5.34 Mechanical property test results for the polypropylene monofilament SDR 7, OLDR 8 and T_{OLHD} = 100°C.

Sample No.	Avg. Diameter (±0.01 mm)	$A_o \times 10^8$ (m^2)	$A \times 10^8$ (m^2)	L_{max} (N)	σ_B (MPa)
1	0.13	1.3	1.0	8.303	830
2	0.13	1.3	1.0	8.346	835
3	0.14	1.5	1.1	8.728	793
4	0.14	1.5	1.2	8.464	705
5	0.14	1.5	1.2	8.926	744

Sample No.	l_o (mm)	Δl_{max} (mm)	Strain (ε_B) (%)
1	30.0	8.670	29.0
2	30.0	9.190	31.0
3	30.0	9.880	33.0
4	30.0	8.250	28.0
5	30.0	9.010	30.0

Sample No.	σ_B (MPa)	ε_B (%)	Slope (L/Δl) (N/m)	Young's Modulus (MPa)
1	830	29.0	2400	5538
2	835	31.0	2400	5538
3	793	33.0	2120	4240
4	705	28.0	2021	4042
5	744	30.0	2708	5415
Avg.	781	30.0	-	4955

Table 5.35 Mechanical property test results for the polypropylene monofilament SDR 7, OLDR 2 and T_{OLHD} = 110°C.

Sample No.	Avg. Diameter (± 0.01 mm)	$A_o \times 10^8$ $(m)^2$	$A \times 10^8$ $(m)^2$	L_{max} (N)	σ_B (MPa)
1	0.17	2.3	1.6	6.668	417
2	0.17	2.3	1.3	6.642	511
3	0.18	2.5	1.4	6.779	484
4	0.18	2.5	1.4	6.733	481
5	0.16	2.0	1.3	6.523	502

Sample No.	l_o (mm)	Δl_{max} (mm)	Strain (ε_B) (%)
1	30.0	12.51	42.0
2	30.0	21.74	72.0
3	30.0	24.28	81.0
4	30.0	24.26	81.0
5	30.0	11.46	38.0

Sample No.	σ_B (MPa)	ε_B (%)	Slope (L/Δl) (N/m)	Young's Modulus (MPa)
1	417	42.0	1976	2578
2	511	72.0	1956	2551
3	484	81.0	3300	3960
4	481	81.0	2462	2954
5	502	38.0	2667	4000
Avg.	479	68.0	-	3209

Table 5.36 Mechanical property test results for the polypropylene monofilament SDR 7, OLDR 4 and T_{OLHD} = 110°C.

Sample No.	Avg. Diameter (± 0.01 mm)	$A_o \times 10^8$ (m^2)	$A \times 10^8$ (m^2)	L_{max} (N)	σ_B (MPa)
1	0.15	1.8	1.4	6.819	487
2	0.16	2.0	1.4	6.872	491
3	0.15	1.8	1.4	7.348	525
4	0.16	2.0	1.5	7.772	518
5	0.17	2.3	1.8	8.413	467

Sample No.	l_o (mm)	Δl_{max} (mm)	Strain (ε_B) (%)
1	30.0	9.970	33.0
2	30.0	11.67	39.0
3	30.0	9.970	33.0
4	30.0	9.650	32.0
5	30.0	8.770	29.0

Sample No.	σ_B (MPa)	ε_B (%)	Slope (L/Δl) (N/m)	Young's Modulus (MPa)
1	487	33.0	3100	5167
2	491	39.0	2667	4000
3	525	33.0	2267	3778
4	518	32.0	3378	5067
5	467	29.0	4000	5217
Avg.	498	33.0	-	4646

Table 5.37 Mechanical property test results for the polypropylene monofilament SDR 7, OLDR 6 and T_{OLDR} = 110°C.

Sample No.	Avg. Diameter (± 0.01 mm)	$A_o \times 10^8$ (m^2)	$A \times 10^8$ (m^2)	L_{max} (N)	σ_B (MPa)
1	0.14	1.5	1.2	8.099	675
2	0.14	1.5	1.2	7.817	651
3	0.14	1.5	1.2	7.831	652
4	0.14	1.5	1.1	7.911	719
5	0.14	1.5	1.1	7.769	706

Sample No.	l_o (mm)	Δl_{max} (mm)	Strain (ε_B) (%)
1	30.0	8.090	27.0
2	30.0	7.700	26.0
3	30.0	8.920	30.0
4	30.0	9.180	31.0
5	30.0	9.800	33.0

Sample No.	σ_B (MPa)	ε_B (%)	Slope (L/Δl) (N/m)	Young's Modulus (MPa)
1	675	27.0	2667	5333
2	651	26.0	2200	4400
3	652	30.0	2311	4622
4	719	31.0	2350	4700
5	706	33.0	2447	4894
Avg.	681	29.0	-	4790

Table 5.38 Mechanical property test results for the polypropylene monofilament SDR 7, OLDR 8 and T_{OLHD} = 110°C.

Sample No.	Avg. Diameter (± 0.01 mm)	$A_o \times 10^8$ (m^2)	$A \times 10^8$ (m^2)	L_{max} (N)	σ_B (MPa)
1	0.14	1.5	1.2	7.490.6.93	624
2	0.13	1.3	1.0	7	694
3	0.13	1.3	1.0	7.128	713
4	0.12	1.1	0.89	6.553	736
5	0.12	1.1	0.88	7.289	828

Sample No.	l_o (mm)	Δl_{max} (mm)	Strain (ε_B) (%)
1	30.0	8.130	27.0
2	30.0	10.82	36.0
3	30.0	10.44	35.0
4	30.0	6.900	23.0
5	30.0	7.650	26.0

Sample No.	σ_B (MPa)	ε_B (%)	Slope (L/Δl) (N/m)	Young's Modulus (MPa)
1	624	27.0	2240	4480
2	694	36.0	1745	4028
3	713	35.0	2000	4615
4	736	33.0	2138	5818
5	828	26.0	2489	6788
Avg.	719	31.0	-	5146

Table 5.39 Mechanical property test results for the polypropylene monofilament SDR 7, OLDR 2 and T_{OLHD} = 120°C.

Sample No.	Avg. Diameter (± 0.01 mm)	$A_o \times 10^8$ (m^2)	$A \times 10^8$ (m^2)	L_{max} (N)	σ_B (MPa)
1	0.18	2.5	1.5	7.302	487
2	0.19	2.8	2.0	7.689	384
3	0.20	3.1	1.7	7.511	442
4	0.18	2.5	1.4	7.001	500
5	0.17	2.3	1.3	7.007	539

Sample No.	l_o (mm)	Δl_{max} (mm)	Strain (ε_B) (%)
1	30.0	18.83	63.0
2	30.0	12.34	41.0
3	30.0	24.10	80.0
4	30.0	21.85	73.0
5	30.0	22.30	74.0

Sample No.	σ_B (MPa)	ε_B (%)	Slope (L/Δl) (N/m)	Young's Modulus (MPa)
1	487	63.0	1867	2240
2	384	41.0	2240	2400
3	442	80.0	2800	2710
4	500	73.0	2556	3067
5	539	74.0	2000	2607
Avg.	470	66.0	-	2605

Table 5.40 Mechanical property test results for the polypropylene monofilament SDR 7, OLDR 4 and T_{OLHD} = 120°C.

Sample No.	Avg. Diameter (±0.01 mm)	$A_o \times 10^8$ (m^2)	$A \times 10^8$ (m^2)	L_{max} (N)	σ_B (MPa)
1	0.14	1.5	1.1	6.784	617
2	0.14	1.5	1.1	6.588	599
3	0.15	1.8	1.3	6.556	504
4	0.15	1.8	1.2	6.293	524
5	0.17	2.3	1.6	7.761	597

Sample No.	l_o (mm)	Δl_{max} (mm)	Strain (ε_B) (%)
1	30.0	9.620	32.0
2	30.0	10.69	36.0
3	30.0	12.49	42.0
4	30.0	13.79	46.0
5	30.0	13.53	45.0

Sample No.	σ_B (MPa)	ε_B (%)	Slope (L/Δl) (N/m)	Young's Modulus (MPa)
1	617	32.0	1733	3467
2	599	36.0	1527	3054
3	504	42.0	2092	3487
4	524	46.0	1886	3143
5	597	45.0	1840	2400
Avg.	568	40.0	-	3110

Table 5.41 Mechanical property test results for the polypropylene monofilament SDR 7, OLDR 6 and T_{OLHD} = 120°C.

Sample No.	Avg. Diameter (± 0.01 mm)	$A_o \times 10^8$ (m^2)	$A \times 10^8$ (m^2)	L_{max} (N)	σ_B (MPa)
1	0.15	1.8	1.4	9.219	658
2	0.14	1.5	1.2	7.393	616
3	0.12	1.1	0.89	7.793	876
4	0.14	1.5	1.2	7.781	656
5	0.14	1.5	1.2	7.903	658

Sample No.	l_o (mm)	Δl_{max} (mm)	Strain (ε_B) (%)
1	30.0	9.010	22.0
2	30.0	6.670	23.0
3	30.0	6.990	26.0
4	30.0	7.840	24.0
5	30.0	7.150	25.0

Sample No.	σ_B (MPa)	ε_B (%)	Slope (L/Δl) (N/m)	Young's Modulus (MPa)
1	658	22.0	2447	4078
2	616	23.0	2545	5091
3	876	26.0	2514	6857
4	656	24.0	2215	4431
5	658	25.0	2353	4706
Avg.	693	25.0	-	5033

Table 5.42 Mechanical property test results for the polypropylene monofilament SDR 7, OLDR 8 and T_{OLHD} = 120°C

Sample No.	Avg. Diameter (± 0.01 mm)	$A_o \times 10^8$ $(m)^2$	$A \times 10^9$ $(m)^2$	L_{max} (N)	σ_B (MPa)
1	0.12	1.1	7.4	6.571	888
2	0.12	1.1	8.9	7.482	841
3	0.13	1.3	11	7.001	636
4	0.13	1.3	10	7.952	795
5	0.12	1.1	9.4	6.317	672

Sample No.	l_o (mm)	Δl_{max} (mm)	Strain (ε_B) (%)
1	30.0	14.81	49.0
2	30.0	6.990	23.0
3	30.0	5.990	20.0
4	30.0	8.180	27.0
5	30.0	5.160	17.0

Sample No.	σ_B (MPa)	ε_B (%)	Slope (L/Δl) (N/m)	Young's Modulus (MPa)
1	888	49.0	2200	6000
2	841	23.0	2514	6857
3	636	20.0	2267	5231
4	795	27.0	2109	4867
5	672	17.0	2000	5454
Avg.	766	27.0	-	5682

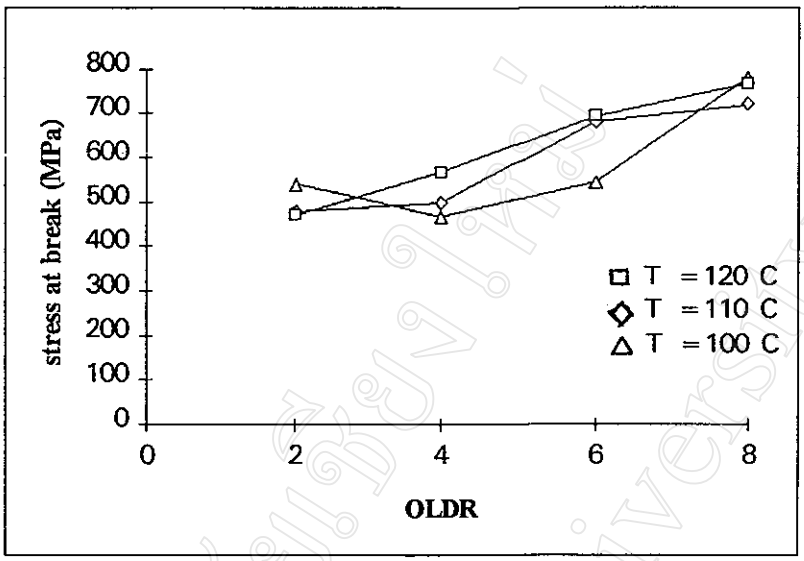

Fig. 5.28 Stress at break of the polypropylene monofilaments as a function of off-line hot draw ratio (OLDR) at three off-line hot drawing temperatures (T_{OLHD}).

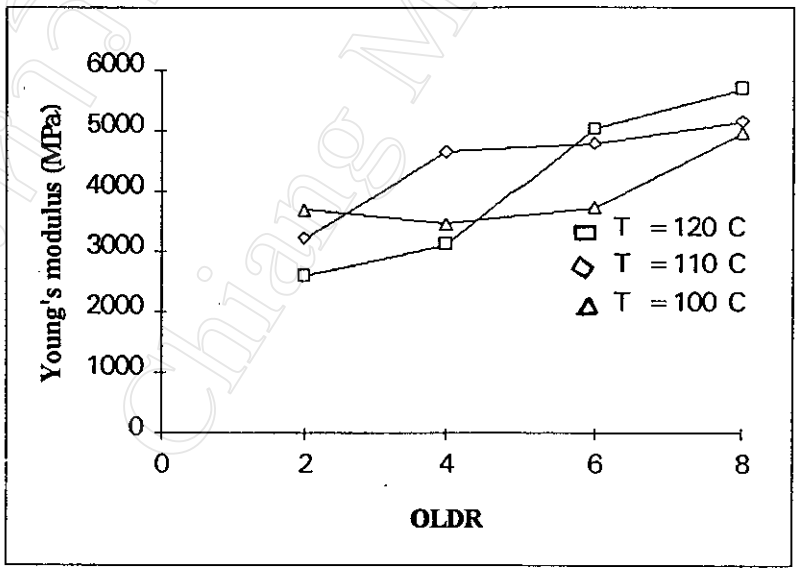

Fig. 5.29 Young's modulus of the polypropylene monofilaments as a function of off-line hot draw ratio (OLDR) at three off-line hot drawing temperatures (T_{OLHD}).

For the synthesized poly(L-lactic acid-co-ε-caprolactone) 8:2 and 7:3 monofilaments, the mechanical property test results are as shown in Tables 5.43 and 5.44.

Table 5.43 Mechanical property test results for poly(L-lactic acid-co-ε-caprolactone) 8:2 monofilament.

Sample No.	Avg. Diameter (± 0.01 mm)	$A_o \times 10^8$ (m^2)	$A \times 10^8$ (m^2)	L_{max} (N)	σ_B (MPa)
1	0.20	3.1	2.5	0.5514	22
2	0.22	3.8	2.8	0.6344	23
3	0.20	3.1	2.4	0.3796	16
4	0.21	3.1	2.4	0.4983	21
5	0.20	3.1	1.4	0.5729	41

Sample No.	l_o (mm)	Δl_{max} (mm)	Strain (ε_B) (%)
1	30.0	7.580	25.0
2	30.0	10.03	33.0
3	30.0	8.330	28.0
4	30.0	28.67	96.0
5	30.0	35.88	120

Sample No.	σ_B (MPa)	ε_B (%)	Slope (L/Δl) (N/m)	Young's Modulus (MPa)
1	22	25.0	557	539
2	23	33.0	978	772
3	16	28.0	800	774
4	21	96.0	857	829
5	41	120	982	950
Avg.	25	60.0	-	773

Table 5.44 Mechanical property test results for poly(L-lactic acid-co-ε-caprolactone) 7:3 monofilament.

Sample No.	Avg. Diameter (± 0.01 mm)	$A_o \times 10^8$ (m^2)	$A \times 10^8$ (m^2)	L_{max} (N)	σ_B (MPa)
1	0.16	2.0	0.56	0.2926	52
2	0.15	1.8	0.55	0.2027	37
3	0.15	1.8	1.3	0.1162	9
4	0.15	1.8	0.52	0.2140	41
5	0.15	1.8	1.1	0.1203	11

Sample No.	l_o (mm)	Δl_{max} (mm)	Strain (ε_B) (%)
1	30.0	76.44	255
2	30.0	68.47	228
3	30.0	10.38	33.0
4	30.0	73.55	245
5	30.0	20.43	68.0

Sample No.	σ_B (MPa)	ε_B (%)	Slope (L/Δl) (N/m)	Young's Modulus (MPa)
1	52	225	400	600
2	37	228	206	335
3	9	33.0	154	260
4	41	245	133	278
5	11	68.0	167	1556
Avg.	30	166	-	606

Finally, in this research project, the three commercial monofilament absorbable surgical sutures were tested. Their mechanical property test results are as shown in Tables 5.45 - 5.49.

Table 5.45 Mechanical property test results for the polyglecaprone 4-0 (Monocryl 4-0) monofilament suture.

Average Linear Density = 61.9 tex

Sample No.	Avg. Diameter (± 0.01 mm)	$A_o \times 10^8$ (m^2)	$A \times 10^8$ (m^2)	L_{max} (N)	σ_B (MPa)
1	0.23	4.5	3.3	27.26	826
2	0.23	4.5	3.3	25.92	785
3	0.23	4.5	3.3	27.18	824
4	0.23	4.5	3.2	27.65	864
5	0.23	4.5	3.2	28.75	898

Sample No.	l_o (mm)	Δl_{max} (mm)	Strain (ε_B) (%)
1	30.0	10.69	36
2	30.0	10.70	36
3	30.0	10.63	35
4	30.0	11.80	39
5	30.0	11.92	40

Sample No.	σ_B (MPa)	Tenacity x 10^2 (N/tex)	ε_B (%)	Slope (L/Δl) (N/m)	Young's Modulus (MPa)
1	826	44.0	36	1304	870
2	785	49.9	36	1167	778
3	824	43.9	35	1500	1000
4	864	44.6	39	1385	923
5	898	46.4	40	1231	820
Avg.	839	45.8	37	-	878

Table 5.46 Mechanical property test results for the polyglecaprone 2-0 (Monocryl 2-0) monofilament suture.

Average Linear Density = 160 tex

Sample No.	Avg. Diameter (± 0.01 mm)	$A_o \times 10^7$ $(m)^2$	$A \times 10^8$ $(m)^2$	L_{max} (N)	σ_B (MPa)
1	0.38	1.1	6.9	60.46	876
2	0.38	1.1	7.2	65.23	906
3	0.38	1.1	7.3	68.19	934
4	0.38	1.1	7.3	68.62	940
5	0.38	1.1	7.0	68.62	982

Sample No.	l_o (mm)	Δl_{max} (mm)	Strain (ε_B) (%)
1	30.0	17.80	60
2	30.0	15.77	52
3	30.0	15.45	52
4	30.0	15.13	50
5	30.0	16.76	56

Sample No.	σ_B (MPa)	Tenacity $\times 10^2$ (N/tex)	ε_B (%)	Slope ($L/\Delta l$) (N/m)	Young's Modulus (MPa)
1	876	37.8	60	2471	674
2	906	40.8	52	2588	706
3	934	42.6	52	3200	873
4	940	42.9	50	3333	873
5	982	42.9	56	2125	580
Avg.	928	41.4	54	-	741

Table 5.47 Mechanical property test results for the poly(glycolic acid-co-trimethylene carbonate) 2-0 (Maxon 2-0) monofilament suture.

Average Linear Density = 185 tex

Sample No.	Avg. Diameter (± 0.01 mm)	$A_o \times 10^7$ (m^2)	$A \times 10^8$ (m^2)	L_{max} (N)	σ_B (MPa)
1	0.40	1.2	7.8	67.65	867
2	0.39	1.2	7.9	67.81	858
3	0.39	1.2	8.2	59.30	723
4	0.39	1.2	8.1	54.01	667
5	0.40	1.2	8.0	66.98	837

Sample No.	l_o (mm)	Δl_{max} (mm)	Strain (ε_B) (%)
1	30.0	16.01	53
2	30.0	15.38	51
3	30.0	13.63	45
4	30.0	14.65	49
5	30.0	15.26	51

Sample No.	σ_B (MPa)	Tenacity $\times 10^2$ (N/tex)	ε_B (%)	Slope (L/Δl) (N/m)	Young's Modulus (MPa)
1	867	36.6	53	12000	3000
2	858	36.6	51	7500	1667
3	723	32.0	45	12000	3000
4	667	29.2	49	12000	3000
5	837	36.2	51	9333	2333
Avg.	790	34.1	50	-	2600

Table 5.48 Mechanical property test results for the poly(p-dioxanone) II 4-0 (PDS II 4-0) monofilament suture.

Average Linear Density = 53.0 tex

Sample No.	Avg. Diameter (±0.01 mm)	$A_o \times 10^8$ (m^2)	$A \times 10^8$ (m^2)	L_{max} (N)	σ_B (MPa)
1	0.22	3.8	2.5	17.18	687
2	0.22	3.8	2.4	16.94	706
3	0.22	3.8	2.5	17.32	693
4	0.23	4.5	2.9	16.54	570
5	0.22	3.8	2.5	17.81	712

Sample No.	l_o (mm)	Δl_{max} (mm)	Strain (ε_B) (%)
1	30.0	16.08	54
2	30.0	16.80	56
3	30.0	16.11	54
4	30.0	16.36	54
5	30.0	16.34	54

Sample No.	σ_B (MPa)	Tenacity $\times 10^2$ (N/tex)	ε_B (%)	Slope ($L/\Delta l$) (N/m)	Young's Modulus (MPa)
1	687	32.4	54	1600	1263
2	706	32.0	56	1667	1316
3	693	32.7	54	1565	1236
4	570	31.2	54	1500	1000
5	712	33.6	54	1500	1000
Avg.	674	32.4	54	-	1163

Table 5.49 Mechanical property test results for the poly(p-dioxanone) II 2-0 (PDS II 2-0) monofilament suture.

Average Linear Density = 139 tex

Sample No.	Avg. Diameter (± 0.01 mm)	$A_o \times 10^7$ (m^2)	$A \times 10^8$ (m^2)	L_{max} (N)	σ_B (MPa)
1	0.36	1.0	5.8	45.58	786
2	0.36	1.0	5.9	45.65	774
3	0.36	1.0	5.8	47.34	816
4	0.36	1.0	5.8	47.30	816
5	0.36	1.0	6.0	48.35	806

Sample No.	l_o (mm)	Δl_{max} (mm)	Strain (ε_B) (%)
1	30.0	21.37	71
2	30.0	20.80	69
3	30.0	21.93	73
4	30.0	21.93	73
5	30.0	20.29	68

Sample No.	σ_B (MPa)	Tenacity $\times 10^2$ (N/d)	ε_B (%)	Slope (L/Δl) (N/m)	Young's Modulus (MPa)
1	786	32.8	71	3556	1067
2	774	32.9	69	3600	1080
3	816	34.0	73	4000	1200
4	816	34.0	73	3467	1040
5	806	34.8	68	4000	1200
Avg.	800	33.7	71		1117

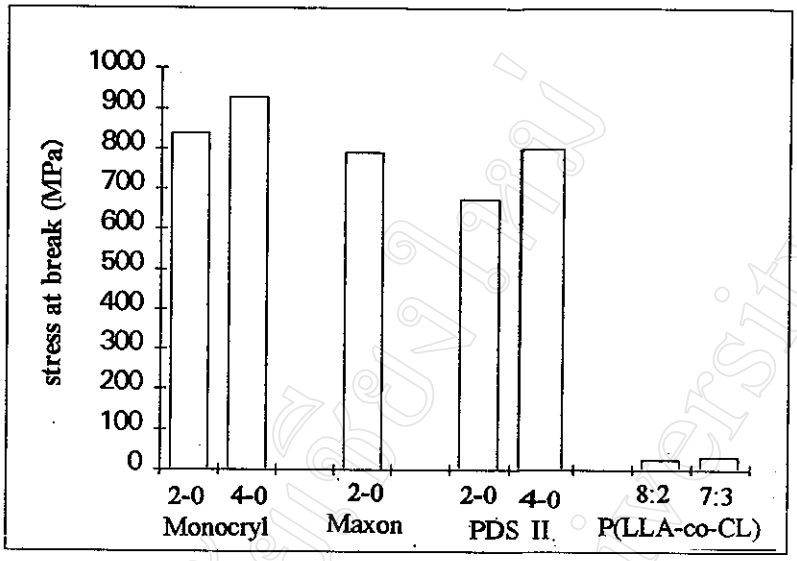

Fig 5.30 Comparison of the stress at break between the commercial monofilament absorbable sutures and the synthesized poly(L-lactic acid-co-ε-caprolactone) monofilaments.

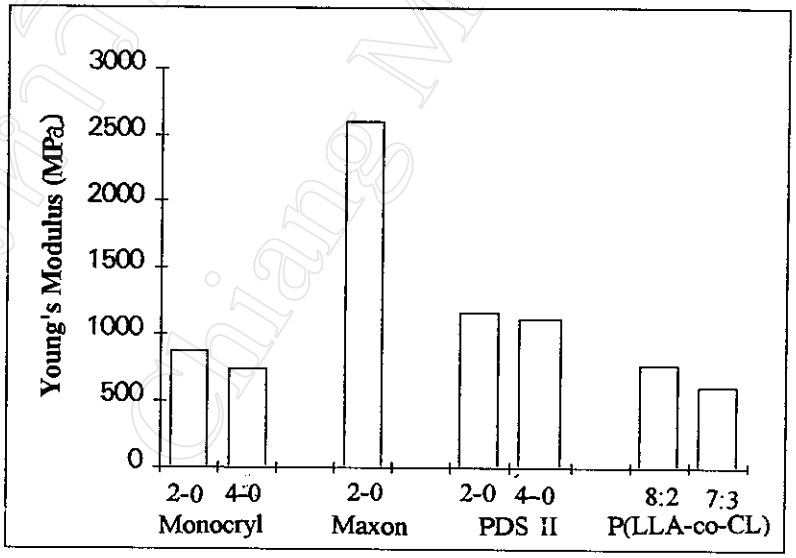

Fig 5.31 Comparison of the Young's Modulus between the commercial monofilament absorbable sutures and the synthesized poly(L-lactic acid-co-ε-caprolactone) monofilaments.

5.9 *In Vitro* Biodegradation of P(LLA-co-CL) Monofilaments

5.9.1 Determination of Weight Loss-Time Profile

An analytical balance was used to accurately weigh the samples. After washing and vacuum drying to constant weight, the % weight retention was calculated as follows:

$$\% \text{ Weight Retention} = \frac{W_f \times 100\%}{W_o}$$

where: W_o = initial weight of sample
W_f = final weight of sample

Table 5.50 Weight loss data for P(LLA-co-CL) 7:3 monofilaments samples immersed in a pH 7.40 phosphate buffer medium at 37.0 ± 1.0°C.

Time (weeks)	P(LLA-co-CL) monofilament weights (± 0.0001 g)		% Weight Retention (± 0.1%)	pH (± 0.01)
	Initial	Final		
0	-	-	100.0	-
1	0.2494	0.2486	99.7	7.40
2	0.2490	0.2464	98.7	7.40
3	0.2494	0.2442	97.9	7.39
4	0.2495	0.2470	98.9	7.39
5	0.2500	0.2425	97.0	7.38
6	0.2497	0.2357	94.4	7.38
7	0.2506	0.2278	90.9	7.35
8	0.2504	0.2209	88.2	7.30
9	0.2494	0.2122	85.1	7.22
10	0.2509	0.2106	83.3	7.15
11	0.2501	0.1019	80.7	7.08

Table 5.51 Comparison of the % weight retentions of the P(LLA-co-CL) 7:3 monofilaments from this study and commercial 'MAXON' monofilament sutures from a previous study [6] following their immersion in a pH 7.40 phosphate buffer medium at 37.0 ± 1.0°C.

Time (weeks)	%Weight Retention (± 0.1%)	
	P(LLA-co-CL) Monofilaments	'MAXON' Sutures
0	100.0	100.0
1	99.7	100.0
2	98.9	100.0
3	97.9	99.8
4	98.9	99.6
5	97.0	98.9
6	94.4	98.2
7	90.9	97.2
8	88.2	95.6
9	85.1	90.4
10	83.9	84.5
11	80.7	80.7

The results in Table 5.50 and 5.51, together with the following Fig. 5.32, combine to show that the P(LLA-co-CL) 7:3 monofilaments are indeed hydrolysable and to an extent similar to commercial 'MAXON' sutures. Although the 11-week immersion period only appears to cover the initial part of the weight loss profile (first 20%), it is enough to provide positive signs that the P(LLA-co-CL) would be biodegradable under physiological conditions if used as a suture material.

The significance of the gradual decrease in pH of the immersion medium is that it confirms the formation and release into solution of low molecular weight degradation products containing acidic (COOH) end-groups.

This is as would be expected from the simple ester hydrolysis mechanism by which polymer biodegradation is belived to occur.

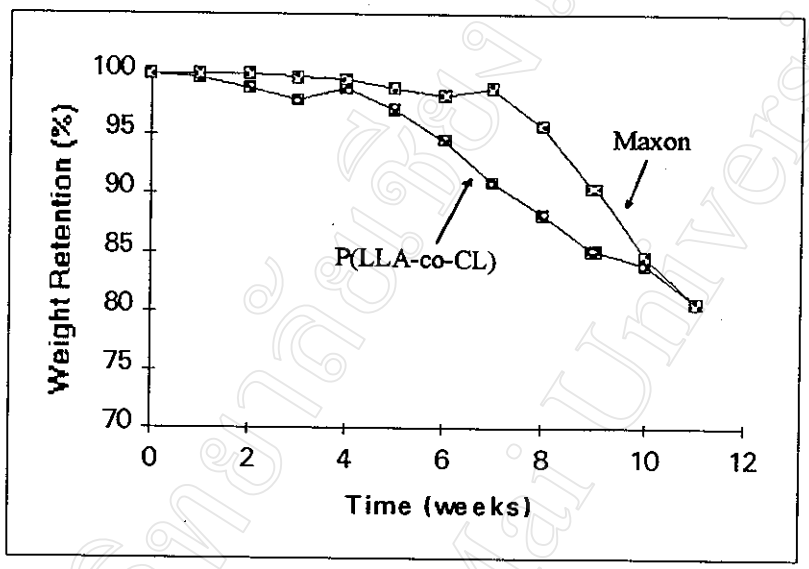

Fig. 5.32 Comparison of the *in vitro* weight loss-time profiles for P(LLA-co-CL) 7:3 monofilaments from this study and commercial 'MAXON' monofilament sutures from a previous study [28].

Immersion medium: pH 7.40 phosphate buffer at 37°C

5.9.2 Melting Point and Heat of Fusion

For each P(LLA-co-CL) sample, DSC analysis of its melting point and heat of fusion gave the results shown in Table 5.52.

Table 5.52 DSC melting peak data for the P(LLA-co-CL) 7:3 monofilaments immersed in pH 7.40 phosphate buffer medium at 37.0 ± 1.0°C.

Time (weeks)	P(LLA-co-CL) 7:3	
	Melting Point (°C)*	Heat of Fusion (J/g)
0	119.44	15.45
1	119.58	19.30
2	119.75	22.53
3	120.48	21.37
4	120.55	21.88
5	121.45	23.76
6	122.43	24.28
7	123.75	25.52
8	124.83	27.42
9	125.94	17.90
10	125.23	27.42
11	125.23	29.10

* taken as the melting peak maximum temperature
scanning rate = 10°C/min
sample size = approx. 3-5 g

Although the changes are relatively small, the melting points and heats of fusion in Table 5.52 do show slight upward trends as the time of immersion increases. This implies an increase in the % crystallinity of the copolymer as hydrolysis proceeds. The explanation for this is that, initially, hydrolysis takes places in the amorphous regions of the matrix into which water can diffuse and gain acess to the hydrolysable ester bonds much more easily. This creates more chain ends which, together with the "plasticising" effect of the water molecules,

facilitates chain mobility resulting in molecular rearrangement and a tendency towards further crystallisation. In addition to this, since initial weight loss takes place from the amorphous regions, it is self-evident that the overall % crystallinity of the remaining matrix must proportionately increase.